T.C.
BAHCESEHIR UNIVERSITY
GRADUATE SCHOOL
THE DEPARTMENT OF BIOENGINEERING

IN SILICO DRUG REPURPOSING OF POTENTIAL SMALL MOLECULE INHIBITOR FOR PSORIASIS TREATMENT: TARGETING INTERLEUKIN-23 WITH VIRTUAL DRUG SCREENING

MASTER'S THESIS

RAGHAD SHARBAJI

ISTANBUL 2024

T.C.
BAHCESEHIR UNIVERSITY
GRADUATE SCHOOL
THE DEPARTMENT OF BIOENGINEERING

IN SILICO DRUG REPURPOSING OF POTENTIAL SMALL MOLECULE INHIBITOR FOR PSORIASIS TREATMENT: TARGETING INTERLEUKIN-23 WITH VIRTUAL DRUG SCREENING

MASTER'S THESIS

THESIS ADVISOR

Asst. Prof. Dr. Pinar SIYAH

ISTANBUL 2024

T.C.

BAHCESEHIR UNIVERSITY

GRADUATE SCHOOL

06/06/2024

MASTER THESIS APPROVAL FORM

Program Name:	BIOENGINEERING PROGRAM
Student's Name and Surname:	RAGHAD SHARBAJI
Name Of The Thesis:	In Silico Drug Repurposing of Potential Small Molecule Inhibitor For Psoriasis Treatment: Targeting Interleukin-23 With Virtual Drug Screening
Thesis Defense Date:	6 June 2024

This thesis has been approved by the Graduate School which has fulfilled the necessary conditions as Master thesis.

Assoc. Dr. Yücel Batu SALMAN

Institute Director

This thesis was read by us, quality and content as a Master's thesis has been seen and accepted as sufficient.

	Title/Name	**Institution**
Thesis Advisor's	Asst. Prof. Dr. Pınar SİYAH	BAHCESEHIR UNIVERSITY
Member's	Asst. Prof. Dr. Alper Devrim ÖZKAN	BAHCESEHIR UNIVERSITY
Member's	Assoc. Prof. Dr. Fırat Barış Barlas	CERRAHPASA ISTANBUL UNIVERSITY

I hereby declare that all information in this document has been obtained and presented in accordance with academic rules and ethical conduct. I also declare that, as required by these rules and conduct, I have fully cited and referenced all material and results that are not original to this work.

Name, Last Name: **RAGHAD SHARBAJI**

Signature:

ABSTRACT

In Silico Drug Repurposing of Potential Small Molecule Inhibitor For Psoriasis Treatment: Targeting Interleukin-23 With Virtual Drug Screening

RAGHAD SHARBAJI

Master's Program in Bioengineering

Supervisor: Asst. Prof. Dr. Pinar SIYAH

Haziran 2024, 87 pages

Interleukin-23 (IL-23) is considered the dominant cytokine in several autoimmune diseases, including psoriasis, a chronic inflammatory skin condition caused by an overactive immune system that attacks healthy skin. The chronic nature of psoriasis could significantly impact the patient's quality of life, with a reduced lifespan of up to 10 years. Despite the effectiveness of available traditional and biological treatments, psoriasis continues to impose significant side effects, highlighting the need for alternative approaches. Small molecule inhibitors (SMIs) targeting IL-23 could be an attractive alternative to current treatments due to their smaller size, oral administration, ease of production, cost-effectiveness, and target specificity. In this research, we aimed to identify the first SMI targeting IL-23 using high-throughput virtual drug screening repurposing techniques. We focused on screening large databases (FDA and Chembridge libraries) on both IL-23 subunits p19 and p40. Molecular docking was performed for all ligands with the two subunits separately. The top 100 docking scored compounds were subjected to molecular dynamic (MD) simulations at 1-ns, 10ns and 100ns. Their binding energies were calculated using MM/GBSA. Then, the binary QSAR analyzes were performed in MetaCore to relate the best candidate small molecules to psoriasis and other skin diseases. As a result, we propose compound Tenapanor as strong inhibitors of p19 and compound with the ChemBridge ID 7740 as strong inhibitors of p40 with favorable properties for psoriasis treatment, further in vitro and in vivo studies are needed to validate these results and consider these IL-23 inhibitors for clinical studies.

Key Words: Psoriasis, IL-23, Small molecule inhibitor, Virtual Screening, Drug Repurposing

ÖZ

Sedef Hastalığına Yönelik Potansiyel Tedavilerin Silico'da Belirlenmesi: Sanal İlaç Taramasıyla Interlukin-23'ün Hedeflenmesi

RAGHAD SHARBAJI
Biyomühendislik Yüksek Lisans Programı
Tez Danışmanı: Asst. Prof. Dr. Pınar SİYAH
Haziran 2024, 87 Sayfa

İnterlökin-23 (IL-23), sağlıklı deriye saldıran aşırı aktif bir bağışıklık sisteminin neden olduğu kronik inflamatuar bir cilt hastalığı olan sedef hastalığı da dahil olmak üzere çeşitli otoimmün hastalıklarda baskın sitokin olarak kabul edilir. Sedef hastalığının kronik doğası, hastanın yaşam kalitesini önemli şekilde etkileyebilir ve yaşam süresini 10 yıla kadar kısaltabilir. IL-23, IL-12 sitokini ile paylaşılan IL-23, p19 ve p40 olmak üzere iki alt birimden oluşmaktadır. Mevcut biyolojik tedavilerin etkinliğine rağmen, sedef hastalığının önemli yan etkileri olmaya devam etmesi, alternatif yaklaşımlara olan ihtiyacı vurgulamaktadır. IL-23'ü hedefleyen küçük molekül inhibitörleri (SMI'lar), daha küçük boyutları, oral uygulamaları, üretim kolaylığı, fiyat/performans etkinliği ve hedef özgüllüğü nedeniyle mevcut tedavilere ilgi çekici bir alternatif olabilir. Bu araştırmada, Yüksek Verimli Sanal ilaç tarama ve ilaç yeniden amaçlandırma tekniklerini kullanarak IL-23'ü hedef alan yeni SMI'ları belirlemeyi amaçlıyoruz. Büyük veri tabanlarını (FDA onaylı ilaçlar ve Chembridge kütüphanesi), hem IL-23p19 hem de p40'ın bağlanma ceplerinde taramaya odaklandık. Kütüphanelerdeki tüm ligandlar için iki alt birime karşı, ayrı ayrı moleküler yerleştirme (Glide/SP) gerçekleştirildi. En iyi yerleştirme puanına sahip ilk 100 bileşik ilk olarak kısa (1-ns) moleküler dinamik (MD) simülasyonlarda (Desmond) kullanıldı. Bağlanma enerjileri MM/GBSA kullanılarak hesaplandı. Daha sonra, en iyi aday küçük molekülleri sedef hastalığı ve diğer cilt hastalıklarıyla ilişkilendirmek için MetaCore'da ikili qsar analizleri yapıldı. Sonuç olarak, p19'un güçlü inhibitörü olarak Tenapanor bileşiğini ve p40'ın güçlü inhibitörü olarak ChemBridge ID 7740 bileşiğini sedef hastalığı tedavisi için olumlu özelliklere sahip aday inhibitörler olarak öneriyoruz. Önerilen IL-23 aday inhibitörlerinin ileride klinik çalışmalarda kullanılabilmesi için detaylı in vitro ve in vivo araştırmalara ihtiyaç vardır.

Anahtar Kelimeler: İlaç yeniden amaçlandırma, sedef hastalığı, IL-23, Moleküler kenetlenme, Moleküler Dinamik (MD) simülasyonu, MM/GBSA

ACKNOWLEDGEMENTS

First of all, I wish to say alhamdulillah “which means praise be to God” in Arabic language for granting me the strength to make this hard-work manageable. Then I would express my sincere appreciation to my supervisor Prof. Dr. Pınar SIYAH for her endless support, valuable advice, constructive criticism, encouragement, kindness, and countless cups of coffee throughout the two years of research. Her mentorship has been invaluable in shaping my academic journey.

I would like to thank my mother, Hana’ a Dalain, for her belief in me and constant support at every step of my life. Additionally, I extend my appreciation to my father, Mohammad Bashar, for his understanding and encouragement for the path I have chosen in life. Indeed, without both, I wouldn’t be the person I am today! Billion thanks to my sisters “Dania and Shahed” and my brothers “Ayman, Ibrahim and Zaid”, I will never forget our online support throughout my master years, the countless hours of chatting, joking, crying, and sometimes even fighting. Special thanks to my 5-years-old twin nieces, Sara, and Maria, for their emotional and psychological support.

Thanks to my family members abroad, who were always there to stand by whenever I wanted and needed them, their endless support was a source of strength and comfort. Special gratitude to Mrs. Sahar Dalain for her delicious cooking and delightful conversations. My thanks also go to the friends who were by my side during this time of my life, I’ll leave your name unmentioned, as you’re well aware of your significance!

Lastly, I'd like to express gratitude to myself for my consistency and patience. These qualities undoubtedly paid off in the end, emphasizing the words of Katalin Kariko: “Persistence always pays off in the end”.

Raghad Sharbaji

TABLE OF CONTENTS

LIST OF TABLES

Tables

LIST OF FIGURES

FIGURES

LIST OF ABBREVIATIONS

2D	Two Dimensiona
3D	Three Dimensiona
ACR20	American College of Rheumatology 20% Response Criteria
ALA	Alanine
ARG	Arginine
ASP	Asparagine
CD	Crohn's Disease
DLQI	Dermatology Life Quality Index
FDA	Food and Drug Administration
HTVS	High Throughput Virtual Screening
IL-23	Interleukin-23
JAK	Janus kinase
MDs	Molecular Dynamics Simulation
MM/GBSA	Molecular Mechanics/ Generalized Born Surface Area
N-terminal	Amino Terminal
NB-UVB	Narrowband Ultraviolet B Radiation
OPLS	Optimized Potential for Liquid Simulations
PASI	Psoriasis Area and Severity Index
PDB	Protein Data Bank
PDB	Protein Databank
PGA	Physician Global Assessment
PsA	Psoriasis Arthritis

PUVA	Psoralen with Ultraviolet A Radiation
QSAR	Quantitative Structure–Activity Relationship Model
RMSD	Root Means Square Deviation
RMSF	Root Means Square Fluctuation
SER	Serine
SMI	Small Molecule Inhibitor
SP	Standard Precision
Th	T-helper
TIP3P	Transferable Intermolecular Potential 3P
TNF-α	Tumor Necrosis Factor Alpha
TOF	Tofacitinib
TYK2	Tyrosine Kinase 2
TYR	Tyrosine
WHO	World Health Organization
XP	Extra Precision

Chapter 1: Introduction

1.1 Introduction

Psoriasis is a chronic inflammatory skin disease that affects 2-4% of the global population (Ma et al., 2023). The World Health (WHO) Organization deems psoriasis as one of the most severe non-infectious diseases. It is associated with hyperproliferative epidermal keratinocytes, self-reactive immune cells, genetic predisposition, and multiple environmental stimuli with clinical symptoms typically presenting as red patches with white scales in areas such as the elbows, knees, scalp, and back which could by extremely painful (Griffiths et al., 2021a; Lønnberg et al., 2013; Lowes et al., 2007; Suzuki et al., 2014). Comorbidities significantly elevated in individuals with psoriasis are psoriatic arthritis, cardiovascular diseases, metabolic syndrome, inflammatory bowel disease, psychiatric disorders, and malignancies (Christophers, 2007; Henseler & Christophers, 1995; Naldi & Mercuri, 2010). However, the mechanisms underlying aberrant keratinocyte behavior in psoriasis are not fully understood. It is widely accepted that multiple factors contribute to the pathological development of psoriasis, but its etiologic is complex and poorly understood (Dopytalska et al., 2021).

Currently, there is no radical cure for this condition. The most used clinical drugs for moderate-to-severe psoriasis are systemic therapy (such as methotrexate and acitretin) and biological agents (such as guselkumab and ixekizumab) (Torres & Filipe, 2015a). However, these drugs have side effects, such as gastrointestinal reactions, bone marrow suppression, and serious liver and kidney damage (Balak et al., 2020; Fiore et al., 2018; Raimondo et al., 2018). Other limitations include the high cost, the need for injection or infusion, and the limited stability and development of antibodies (Dodson & Lio, 2022; Feldman, Goffe, et al., 2016). There is a need to develop more effective and safer therapies for psoriasis, with small-molecule (SMIs) inhibitors showing superior therapeutic effects for various diseases, including psoriasis. Due to their benefits, including their small size, oral administration, ease of production, cost-effectiveness, mild-to-moderate side effects, lack of genetic interference, easily modified structure, and target specificity. SMIs have led to an expansion of their use in

psoriasis treatment as alternatives to systemic therapy and antibody biologic drugs (Megino-Luque et al., 2020; Torres & Filipe, 2015a).

Curent investigation focuses on interleukin-23 (IL-23) small molecule inhibitors. IL-23 is recognized as the dominant cytokine controlling inflammation in peripheral tissues and joints and is associated with several autoimmune diseases, including psoriasis (Tang et al., 2012). It is a key regulator for many cytokines and generated by monocytes, myeloid dendritic cells, and macrophages. IL-23 acts on T helper cells via IL-12Rβ1, IL-23Rα receptors and intracellular JAK–STAT- the transmembrane receptor complex-, triggering a cascade of intracellular signals (IL-17A, IL-17F, and IL-22) and stabilizing, activating, and enhancing the cytokine production of IL-17-producing lymphocyte cells (Song et al., 2021; Thakur et al., 2023). Research indicates that blocking IL-23 shows promising results in treating psoriasis, referred to the well tolerated agents of IL-23 (P19 & P40), highly effective (achieving a 90% reduction in the psoriasis area), and associated with mild-to-moderate side effects (Dodson & Lio, 2022). Ongoing clinical trials of available anti-biologic drugs suggest that targeted IL-23 inhibitors for psoriasis treatment may offer more sustained long-term efficacy compared to targeted IL-12, IL-17, and IFN therapies (Yang et al., 2021). Ustekinumab and briakinumab are the first FDA-approved anti-IL-12/23 drugs, blocking the shared P40 subunit in IL-12/23, and are used to treat moderate to severe psoriasis. While these drugs have shown effectiveness and disease reduction, they share common limitations with other antibody biologic drugs, as we mentioned early (Colquhoun & Kemp, 2024; Parigi et al., 2022).

Here, our research aims to repurpose available drugs – FDA library of approved drug and clinical investigation compounds - for treating moderate to severe psoriasis by discovering small molecule inhibitors of IL-23. To achieve this, an in-silico approach consisting of high throughput virtual screening was applied. First, small molecule libraries were screened for binding affinity to the crystal structure of the p19 and p40 subunits of IL-23. Then, a combination of molecular docking and molecular dynamics (MD) simulations across different timescales were employed to refine the binding poses and further evaluate the stability of the protein-ligand complexes. To further explore the mode of action of the small molecule inhibitors, and ensure the

stability of protein-ligand complexes, additional in silico studies were performed to gain insight into the binding mechanisms of the small molecules. Free energy calculations (MM/GBSA) that resulted from calculating the average energy of the frames during the 100ns simulation was calculated to estimate the binding affinity and stability of the small molecules and to identify key residues involved in their binding to IL-23. QSAR analyzes was performed in MetaCore platform to relate the best candidate small molecules to psoriasis and other skin diseases.

1.2 Purpose of the Study

The objective of this study is to discover small molecule inhibitors targeting both p19 and p40 subunits of IL-23 for treating moderate to severe psoriasis. Given the central role of IL-23 in driving the inflammatory response in psoriasis, targeting this interleukin presents a promising therapeutic approach. Our goal is to enhance IL-23 target specificity, minimize side effects, reduce dosing frequency, and increase drug efficiency by utilizing in silico approaches, which involve computational methods for drug discovery and optimization. By leveraging available small molecule libraries and repurposing them to treat psoriasis, we will employ high-throughput screening approaches, including docking, molecular dynamic simulations, MM/GBSA analysis, and QSAR analyzes performed in MetaCore to identify the most effective drug candidates that directly target and suppress IL-23. The identification of lead compounds will necessitate in-vitro and in-vivo studies to validate the in-silico results. Beyond psoriasis treatment, successful development of IL-23 SMIs could have broader implications for the treatment of other autoimmune disease where IL-23 plays a pivotal role, ultimately revolutionize psoriasis treatment, and improving patient's quality of life.

Chapter 2: Literature Review

2.1 Psoriasis Disease

Psoriasis is an autoimmune chronic disease that effect the healthy skin occurring worldwide where it effects over than 60 million individuals around the world and the lifetime prevalence of psoriasis increases over the decades where it increased by 26.53% over the last three decades (1990-2019) (Is Psoriasis Becoming More Common?, 2024; Psoriasis - ScienceDirect, n.d.). The world health organization describes psoriasis as "chronic, non-communicable, painful, disfiguring, and disabling disease for which there is no cure"(Griffiths et al., 2021a). psoriasis is characterized by raised, scaly, and itchy skin lesions over the extensor surfaces, scalp and lumbosacral region (Gulliver et al., 2018; Nair & Badri, 2024).

The pathogenesis of psoriasis is complicated, multigenic and multifactorial. Genetics plays a kay role (The largest contributor) in the disease occurrence with other environmental triggers such as obesity, stress and smoking (Griffiths et al., 2021b; Man et al., 2023). Where cells like T cells, dendritic cells and keratinocytes consider key players in psoriasis with the IL-23/ Th17 axis being the core activators of immune system. The simplest way to describe the psoriasis mechanism is when activation of different types of dendritic cells lead to the production of tumor necrosis factor alpha (TNF-α), IL-12, and IL-23 which enhance the activation of T helper 1 (Th1) and Th17. Following by the secretion of many inflammatory cytokines like IL-17, IL22 and TNF-**α,** where they activate the keratinocyte cells to produce cytokines, chemokines and antimicrobial peptides and to initiate the inflammation (Man et al., 2023; Zhou et al., 2022).

Psoriasis has many clinical types which are plaque (the most common) psoriasis, inverse, guttate, pustular or erythrodermic psoriasis and Nail pitting (Figure1). They are all differ on the psoriasis location, the form of scale and the severity of the disease (Nair & Badri, 2024). Psoriasis's patients are in high risk to develop other diseases such as psoriasis (PsA) arthritis, obesity, cardiovascular and liver disease, diabetes, inflammatory bowel disease, Crohn disease, and rheumatoid arthritis. Not to mention the increasing rate of different mental disorders compering with the general population. The consequence is an elevated mortality rate due to the mentioned

comorbidities (Christophers, 2007; Man et al., 2023). Different kind of treatments could be used depend on the psoriasis severity (assessed with the Psoriasis Area and Severity Index [PASI], which ranges from 0 to 72 [most severe disease]), location, patient's age and the effect of psoriasis on the patient's quality of life (assessed by the Dermatology Life Quality Index [DLQI], which range from 0 to 30 [large impact]) (Ghoreschi et al., 2021). Mild psoriasis treatment options include topical therapy (vitamin D or corticosteroids) and phototherapy as a second-line therapy (narrowband ultraviolet B radiation (NB-UVB) and psoralen with ultraviolet A radiation (PUVA)). Moderate to severe psoriasis treatment includes systematic medications or chemically synthesized immunosuppressive (Methotrexate and acitretin), biologics, modern small molecules, oral agents and phototherapy (Armstrong & Read, 2020; Gulliver et al., 2018).

Figure 1. a, b Plaque Psoriasis, c, d Guttate Psoriasis, e Inverse Psoriasis, f Erythrodermic Psoriasis, g Pustular Psoriasis, h Nail Pitting, i Psoriatic Arthritis (Guo et al., 2023).

Improved understanding of psoriasis pathogenesis has fuelled the development of novel therapies in recent decades. Among these, biological treatments have revolutionized psoriasis management due to their superior safety and efficacy compared to traditional approaches (Jiang et al., 2023). Biological therapy is utilized targeted agents to modulate specific components of the immune system or downstream effector pathways (Sivamani et al., 2010). Biologics are large and heterogeneous molecules, produced inside the living cell, rather than using non-living vessels, and include things like hormones, vaccines, blood products, and monoclonal antibodies (Makurvet, 2021). Here, we present a review of the commonly used biological treatments targeting distinct mechanisms in psoriasis. They are categorized into three groups, IL-23 inhibitors, TNF-α inhibitors, and IL-17 inhibitors.

2.2 TNF-α Inhibitors

FDA-approved TNF-α inhibitors have emerged as a powerful force in treating moderate to severe psoriasis. Etanercept, adalimumab, and infliximab have become the dominant in this area. Certolizumab and golimumab are additional TNF-α inhibitors, but their use in psoriasis remains under investigation (Chima & Lebwohl, 2018). Two double-blind, placebo-controlled studies demonstrate that patients with psoriasis achieved significant improvement (PASI 75) within three months of Etanercept subcutaneous injection. Etanercept has shown superior efficacy for psoriasis patients with concurrent psoriasis and psoriatic arthritis, according to the American College of Rheumatology 20% response criteria (ACR20). Similar benefits are observed with other TNF-α inhibitors; however, selecting the optimal therapy depends on individual patient characteristics (Chima & Lebwohl, 2018; Jiang et al., 2023). For instance, infliximab might be the preferred course for overweight patients with psoriasis due to its potential for achieving superior PASI 75 response and boosting dermatology life quality index scores. Adalimumab and infliximab might be better for psoriasis patients with Crohn's disease (CD)(Jiang et al., 2023).

While TNF-α inhibitors are a valuable treatment for many conditions, they can cause adverse effects. The most common ones are increased risk of infections (eg. upper respiratory sinusitis), tuberculosis, headaches and rashes, infusion reactions, lupus like

syndrome, abdominal pain, and injection side reaction (Chima & Lebwohl, 2018; Kamata & Tada, 2020; Sivamani et al., 2010).

2.3 IL-17 Inhibitors

IL-17 inhibitors have emerged as a powerful tool in managing moderate to severe psoriasis. Three FDA-approved IL-17 inhibitors- Ixekizumab, secukinumab, and brodalumab- offer patients effective options. Additionally, bimekizumab and natakimab are promising inhibitors currently under clinical trials. Robust clinical data supports the efficacy of IL-17 inhibitors (Hohenberger et al., 2018; Mosca et al., 2021). Randomized, double-blind, placebo-controlled phase III by (Lebwohl et al., 2020) demonstrated ixekizunab's superiority over placebo and etanercept (a TNF-α inhibitor) in achieving and maintain high levels of efficacy for up to 4 years of treatment. On the long term of treatment, brodalumab was significantly more officious, effective, and skin clearance than secukinumab, ixekizumab, etanercept and ustekinumab (IL-23 inhibitor). A 2019 systematic review by Sawyer (Sawyer et al., 2019) highlights the potential benefits of both brodalumab and ixekizumab compared to all TNF- α, with etanercept showing the least expected long term efficacy.

The most frequent side effects associated with IL-17 targeted therapy include nasopharyngitis, upper respiratory tract infection, injection site reaction, headache, diarrheal, arthralgias, candida infections. While a black box warning for suicidal behavior was initially issued for brodalumab, subsequent evaluations revealed no causal link, and warning was cancelled (Mosca et al., 2021).

2.4 IL-23 Inhibitors

Ustekinumab and Briakinumab are the FDA approved inhibitors of the shared p40 subunit between IL23 and IL-12, which impacts the signalling of both. Among the inhibitors of IL-23p19 are Tildrakizumab, Guselkumab, Risankizumab, and Mirikizumab (Ghazawi et al., 2021). Ustekinumab as an example had a considerably higher PASI 90 compared to etanercept (Griffiths Christopher E.M. et al., 2010).It has been discovered that ustekinumab continues to be effective after continuous use for at least five years according to three separate trials (PEARL, Igarashi, LOTUS) on patients in Asia, which All trials showed positive results for the treatment of psoriasis (Igarashi et al., 2012; Tsai et al., 2011; Zhu et al., 2013). Guselekumab showed a stable safety

profile in several clinical trials, such as X-PLORE, VOYAGE, ECLIPSE, a Japanese Phase III trial, NAVIGATE, and ORION investigations. In treating psoriasis, it had strong effectiveness and was typically well-tolerated comparing with other biologics (Figure2)(Blauvelt et al., 2017; Langley et al., 2018; Reich, Armstrong, et al., 2017).

Tildrakizumab showed better efficacy and tolerancy than placebo and etanercept according to a phase 2b study was published in 2015 (Reich, Papp, et al., 2017). Nevertheless, there were no parallel studies conducted using ustekinumab and TNF-α inhibitors. The major advantages of IL-23 inhibitors is the less frequent dosing compared to IL-17 and TNF-α with no risk of inflammatory bowel disease or increased risk of candidiasis (Yang et al., 2021). Generally, IL-23 and IL-17 inhibitors have been shown to work better than more traditional oral medications and biologics. Particularly, when compared to ustekinumab, adalimumab, certolizumab, and etanercept, infliximab, ixekizumab, secukinumab, bimekizumab, brodalumab, risankizumab, and guselkumab were proven to be more effective in reaching PASI 90 (Sbidian et al., 2023).

The most frequent side effects associated with IL-23 targeted therapy include upper respiratory tract infection, nasopharyngitis, arthralgia, headache, back pain, diarrhea, and injection site erythema, serious infections were rare with no unexpected safety findings after years of IL-23 inhibitor treatments (Yang et al., 2021).

Figure 2. A 27-Year-old Male with Erythematous-Desquamative Plaques on His Back had Moderate-to-Severe Psoriasis (A). After 12 Weeks of Treatment with an IL-23 Inhibitor, he Achieved Complete Skin Clearing (B) (Bellinato et al., 2021).

2.5 Safety Concerns of Biologics

The development of biologics has revolutionised psoriasis treatment, improving efficacy and safety under appropriate supervision. Compared to TNF-α inhibitors, biologics like IL-17 inhibitors and anti-IL-12/23 antibodies typically exhibit less severe side effects. On the other hand, IL-17 inhibitors can cause inflammatory bowel disease and candidiasis, while TNF-α inhibitors carry a risk of significant infections and infusion responses. As of yet, no particular side effects have been documented with IL-23 inhibitors (Kamata & Tada, 2018). Long-term safety data are still required, especially because immunogenicity and the chronic nature of psoriasis are factors that may affect how well a treatment works over the long run. Present biologic treatments do not raise the risk of malignancy, even though people with psoriasis have greater incidence of malignancy. It is recommended that healthcare professionals be up to date on the most recent advancements in psoriasis biologic therapy (Kamata & Tada, 2020).

2.6 Cost and Accessibility

Taking Adalimumab as an example of biologic drug, and due to its great efficacy in treating diseases like psoriasis and rheumatoid arthritis, sales and price have skyrocketed, reaching $18.9 billion in 2017 and maybe as high as $15.2 billion by 2024 (Rowland, 2020; Turner, 2018). Even when the patent expired in 2016, additional patents kept the company dominant in the market, driving up prices to almost $72,000 year. This circumstance draws attention to an imbalance in patient access, since most patients cannot afford biologics due to their high cost of development and their effectiveness, which drives up their pricing in the pharmaceutical business. Although the company's profit financially from these high charges, fewer individuals are able to pay these treatments. Since health care is a vital necessity, it is important to strike a balance between drug profitability and accessibility and cost (Makurvet, 2021).

Then, because of the need to make sure that a wider range of patients may receive effective medications, there is a movement towards developing more accessible and affordable treatments for psoriasis. This change is stimulating the investigation of novel treatment options, like ***small molecule inhibitors.*** As a first step, in 2017, biologics accounted for barely 2% of US prescriptions, yet 37% of all small molecules spent in the nation (*Medicine Use and Spending in the U.S.*, n.d.) and the FDA approved small

molecule inhibitor were the doubled of biologics from 2010 to 2017 (Figure 3). Differences in the production and properties of biological substances and small molecules greatly affect their costs and thus their availability to consumers. Despite the remarkable success of biologic drugs in healthcare, the issue of availability remains a concern, as the high cost of these drugs often limits their availability to end users. This ongoing challenge underscores the need for a balanced approach to drug development that considers both innovation and patient access (Declerck et al., 2010; Makurvet, 2021).

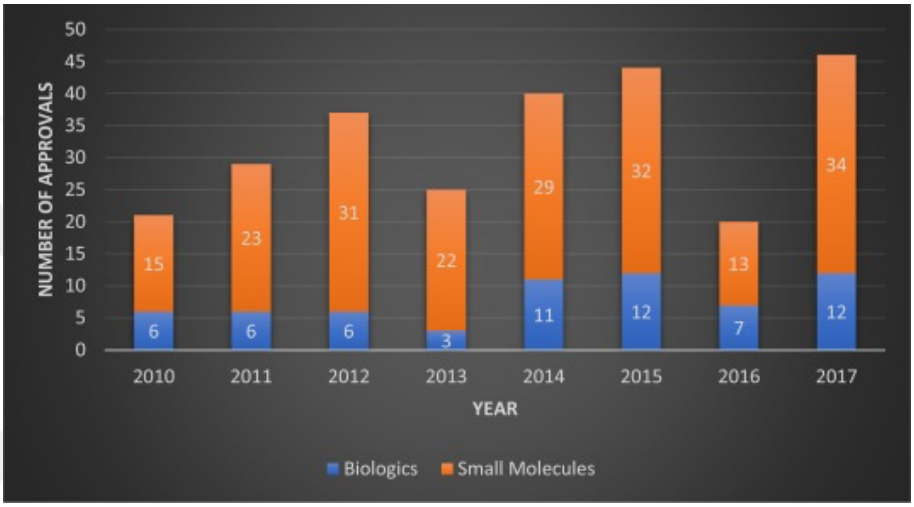

Figure 3. FDA Approvals for Biologics and Small Molecules from 2010 to 2017 (Medicine Use and Spending in the U.S., n.d.).

2.7 Small Molecule Inhibitors as an Alternative to Biologic Inhibitors

Small-molecule inhibitors (SMIs) are a class of novel therapies that are prized for their low molecular weight, which makes them easy to enter cells. They are compounds with a size of less than 1000 Da and are typically administered orally. SMIs are designed to target specific molecules, regardless of their cellular location. In the recent decades, targeted SMIs have emerged as a superior therapeutic approach for various diseases, including cancer and autoimmune diseases (Megino-Luque et al., 2020). In psoriasis treatment, the use of SMI has demonstrated an alternative option to systemic therapy and antibody biologic drugs, particularly for individuals who are no longer responding to targeted or conventional antibody treatments. They offer several

benefits, including their ease of production, cost-effectiveness, mild-to-moderate side effects, lack of genetic interference, easily modified structure structures, and target specificity (Torres & Filipe, 2015a). Scientists have developed several SMIs to treat psoriasis and other autoimmune diseases. Such as Deucravacitinib, apremilast, dimethyl fumarate, and tofacitinib (Bellinato et al., 2021; Camela et al., 2021).

2.8 Deucravacitinib

Is a small molecule (425.5 Da) (PubChem, n.d.) and the first oral Tyrosine kinase 2 TYK2 Inhibitor (BMS-986165) for Moderate to Severe Plaque Psoriasis to receive FDA Approval (Truong et al., 2024). By selectively binding to the regulatory domain of TYK2, deucravacitinib exhibits more selective efficacy as compared to other Janus kinase (JAK) inhibitors that compete with ATP. It specifically targets the type 1 interferon, IL-23, and IL-12 pathways, which are essential to the etiology of psoriasis (Bellinato et al., 2021). In a long-term extension study, an average of 65.1% of participants in this trial had reduced their Psoriasis Area and Severity Index by more than 75%, or a PASI 75 response by week 16. A greater percentage of patients receiving deucravacitinib 6 mg once daily achieved PASI 75 (Truong et al., 2024). As a result of its consistent effectiveness and safety profile, decraceditinib has been approved for use in adult patients with moderate to severe plaque psoriasis who are suitable for systemic treatment or phototherapy (Jin et al., 2023). Nasopharyngitis, headaches, diarrhea, nausea, upper respiratory tract infections, and acne were the most frequently reported side effects; the latter was more common in the deucravacitinib group (Roskoski, 2023; Truong et al., 2024).

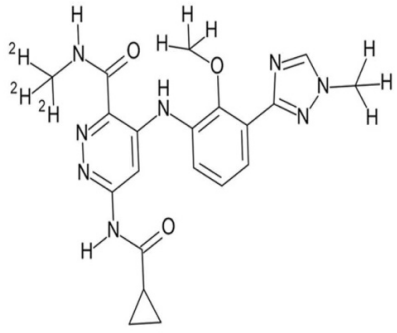

Figure 4. 2D Structure of Deucravacitinib.

2.9 Apremilast

Apremilast is another small and oral FDA approved inhibitor, that blocks the phosphodiesterase-4 (PDE4), Its effect downregulates the production of IL-23, IL-17 and TNF-α cytokines and raises cyclic AMP (cAMP) levels in inflammatory cells. In a wide range of studies including (Phase III/IV Studies, Liberate, Unveil, Real life and Style studies) showed that after of 16 weeks of Apremilast treatment, nearly half of the patients achieved significant scalp clearance, with sustained results through weeks 52 and 104. The STYLE study specifically noted significant improvements by week 16 in patients who had not responded to topical therapies. Additionally, apremilast appears to reduce skin proliferation, epidermal thickness, and psoriasiform reactions (Hansen & Kavanaugh, 2014; Ogdie et al., 2020) . Apremilast was generally well tolerated in these studies; the most frequent side effects were mild to moderate and included headaches, nausea, nasopharyngitis, and diarrhea. Apremilast's good safety profile was confirmed by the absence of any new serious adverse events or appreciable changes in test results throughout numerous clinical trials (Camela et al., 2021; Torres & Filipe, 2015b).

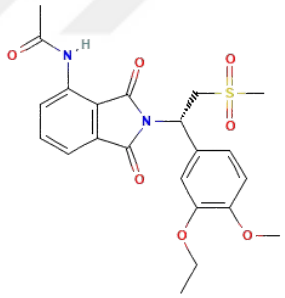

Figure 5. 2D Structure of Apremilast.

2.10 Tofacitinib

A small and oral Janus kinase (JAK) inhibitor is being studied to treat inflammatory diseases. The pathway controlling inflammation is composed of JAK proteins, including JAK1, JAK2, JAK3, and TYK2. Tofacitinib (TOF) was first approved for rheumatoid arthritis in 2012 and then psoriasis in 2017 (Tian et al., 2019). Due to an increased risk of side effects, TOF has not been authorized for long term psoriasis therapy. Two large-scale phase III trials (NCT01276639 and NCT01309737)

assessed tofacitinib at doses of 5 mg and 10 mg twice day, over a duration of 16 weeks. Patients were followed up on for 52 weeks during the research, after which those who did not show enough progress by week 28 were dropped. When compared to the placebo group, the tofacitinib groups' PASI 75 and Physician Global Assessment (PGA) scores significantly improved by week 16, with the effects being more pronounced for the higher 10 mg dose (Caputo et al., 2021; Tian et al., 2019). According to another research conducted on Japanese patients, tofacitinib greatly reduced psoriasis symptoms, with faster effects becoming apparent by week 4 for higher dosages. In a different study, tofacitinib 10 mg twice day was found to be equally efficacious but had a faster onset of action than etanercept during a 12-week period (Feldman, Thaçi, et al., 2016; Papp et al., 2015).

Tofacitinib was generally well tolerated in these studies; the most frequent side effects were Nasopharyngitis, upper respiratory tract infection, headache, diarrhea, vomiting, nausea (Berekmeri et al., 2018). Overall, tofacitinib presents a potentially useful oral treatment alternative for psoriatic disease patients who have not responded well to prior treatments and who would rather take medication orally rather than intravenously (Bissonnette et al., 2015; Griffiths et al., 2017).

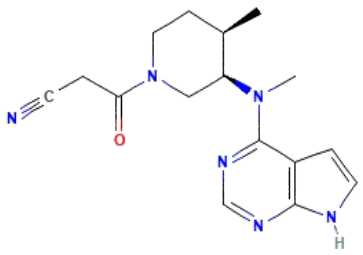

Figure 6. 2D Structure of Tofacitinib

2.11 Safety Concerns and accessibility of small molecule inhibitors

Small molecules —including JAK, PDE4 inhibitors and others— considers as the next generation of psoriasis treatment. These therapies have several benefits, including the ability to be applied topically or orally instead of intravenously, a decreased chance of immunogenic reactions, and generally reduced costs.

Consequently, in comparison to biologics, they are more widely available and financially feasible. Small molecules are becoming a more popular choice for many patients due to their price and simplicity of administration, even if biologics are frequently more effective for specific illnesses (Cascella et al., 2016).

Furthermore, medical treatment development should not only focus on scientific breakthroughs, but also on improving patient accessibility and affordability, ensuring that advances in healthcare benefit all members of society. Because of biologics large size and complex structure, they are susceptible to production variability, which can result in unpredictable immunogenic responses. Small molecules, such as aspirin and varenicline, are chemically synthesized; they are smaller, simpler in structure, stable, and non-immunogenic (Makurvet, 2021).

Early results are encouraging, but more investigation is required to completely determine their safety and effectiveness. These small compounds may provide brand-new approaches to the treatment of psoriasis since they seem to efficiently target cutting-edge immune pathways. This emphasizes how crucial it is to keep funding various forms of medication development in order to satisfy the wide range of patient needs (Torres & Filipe, 2015b).

2.12 Why IL-23 as targeted cytokine?

The cytokine interleukin-23 (IL-23) is a heterodimeric member of the IL-6 family that consists of two subunits: p19 and p40. The latter is also a part of IL-12. While p19 is organized as a four-helix bundle cytokine, the p40 component is composed of three domains (D1, D2, and D3) (*Cytokine Frontiers*, n.d.; Pastor-Fernández et al., 2020). Studies using genetically engineered mice have shown that IL-23 is essential for the aggravation of autoimmune disorders, mainly through encouraging the growth of T cells that produce IL-17 (Cua et al., 2003). On the other hand, a decreased risk of certain autoimmune disorders in humans, such as multiple sclerosis, psoriatic arthritis (PsA), and psoriasis, has been linked to a lack of IL-23 (Langrish et al., 2004; Teunissen et al., 1998).

IL-23 is especially active in the joints (Sherlock et al., 2012) and at barrier surfaces like the skin and stomach (Chan et al., 2006; Yen et al., 2006). The interconnectedness of these illnesses can be shown by the increased likelihood of

exhibiting signs of a linked disease at any one of these locations. For example, the clinical presentations of Psoriasis and PsA are closely associated with IL-23-driven inflammation in the gut, skin, or joints (Scher et al., 2015). When IL-23 binds to its receptor, IL-23R, it stimulates many signaling pathways on different immune cells including Janus kinases (JAKs), and signal transducers and activators of transcription (STATs) which upregulating the Th17 cell-specific genes, ultimately leading to inflammatory response. This interaction highlights how important IL-23 is to the pathophysiology of psoriasis, indicating that it is an important cytokine involved in the regulation of inflammation and immune responses in these conditions (Chan et al., 2006; Sherlock & Cua, 2021; Yen et al., 2006).

In addition to being very effective—studies have shown that some patients have experienced a 90% reduction in psoriatic area—IL-23 inhibitors also have a favorable safety profile, with most side effects being mild to moderate (Dodson & Lio, 2022). Psoriasis can be targeted with IL-23 inhibitors because they block the IL-23-IL-17 pathway, which is a major factor in the development of the disease. In contrast to other biologic therapies that target TNF-alpha, IL-17, and IL-12/23, preliminary data indicates that IL-23 inhibitors may have more durable efficacy. These drugs also show encouraging pharmacokinetic qualities in mice, which means the body absorbs and uses them efficiently (Cua et al., 2003; Yang et al., 2021).

As we mentioned earlier, there are currently several IL-23 inhibitor medications on the market, such as ustekinumab, guselkumab, tildrakizumab, Risankizumab, and mirikizumab (some of them we have already covered). Numerous studies show that there is little chance of serious side effects when taking these drugs. Despite encouraging studies, IL-23 inhibitors are still regarded as a relatively new class of pharmaceuticals. Additional research is being conducted to confirm their long-term safety and effectiveness. Furthermore, additional clinical information is required to completely comprehend their potential advantages over alternative psoriasis treatments (Sherlock & Cua, 2021).

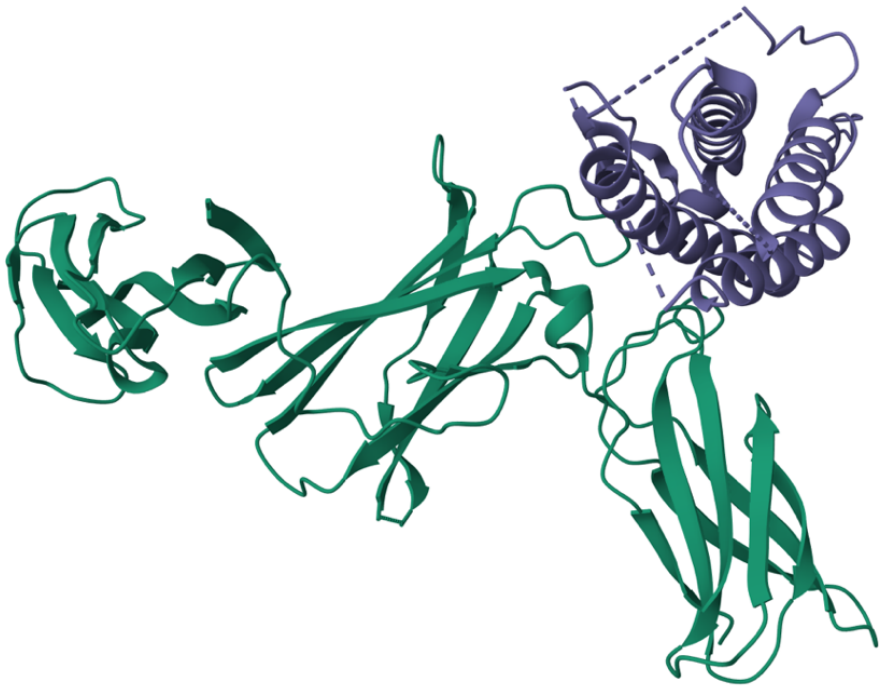

Figure 7. IL-23 (PDB:3DUH)

Chapter 3: Methodology

3.1 Introduction

This research was aimed at identifying promising inhibitors for the IL-23p19 and IL-23p40 subpopulations of cytokine, through a comprehensive examination of over million and half molecules from FDA (https://www.fda.gov) and ChemBridge databases (https://chembridge.com). Several computational methods were used in the study, which was systematically guided by a workflow designed for efficiency and effectiveness. The process began with the preparation of the IL-23p19 and IL-23p40 proteins for docking, utilizing Schrödinger-Maestro's Protein Preparation Wizard tool (Madhavi Sastry et al., 2013). Based on literature reviews, grid box has been generated for both subunits to set the molecular docking.

Using the Schrödinger Maestro LigPrep tool, ligands from FDA and ChemBridge databases have been prepared for a virtual screening (Chen & Foloppe, 2010). The docking of IL-23p19 with Glide/SP against each database was started separately (Friesner et al., 2004; Halgren et al., 2004). This was followed by a 1ns molecular dynamic simulation (MDs) for the top 100 docking scores complexes (Bowers et al., 2006) and MM/GBSA calculations (Li et al., 2011) to filter complexes based on their MM/GBSA scores. A further 10ns MD simulation followed by another round of MM/GBSA calculations was carried out on the top 10 compounds with the lowest scores. Another simulation of 100ns MD was performed on the highest five compounds with the lowest score, and then a second round of MM/GBSA calculations resulted in four promising hit inhibitors for IL-23p19. In the case of IL-23p40, a similar approach resulted in four promising hit inhibitors too.

The top compounds selected from the 100-ns MD and MM/GBSA analyses of IL-23 subunits P19 and P40, derived from the FDA and ChemBridge databases, were submitted to QSAR models on the METACORE™/METADRUG™ platform. This was done to predict the biological activity of the promising compounds and ensure that the predicted activities aligned with the dynamic behavior observed in the simulations. These findings were then compared with a control group containing three small molecule inhibitors that indirectly target IL-23. Docking studies of these inhibitors with both IL-

23p19 and IL-13p40, followed by 1-ns and 100-ns MD simulations, were conducted for comparative analysis.

This comprehensive methodology relies on the use of cutting-edge computer technologies in identifying possible inhibitors that are highly effective at neutralizing IL 23 in order to seek new treatments for conditions such as psoriasis. A schematic diagram of Figure 8 shows the full methodology.

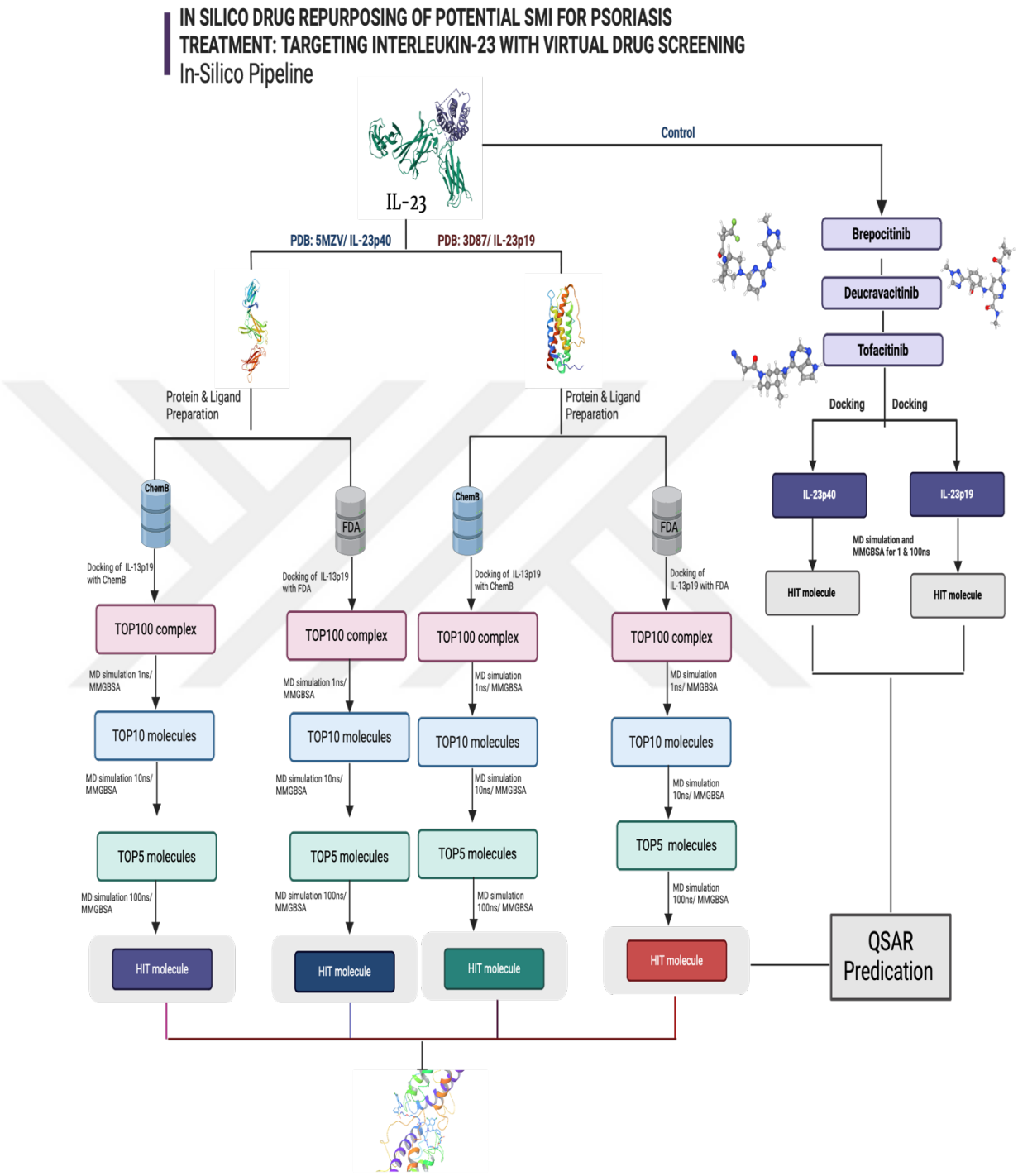

Figure 8. Schematic Representation of the Complete Method for the Discovery of IL-23 Inhibitor.

3.2 Structural preparation of IL-23

IL-23 is a pivotal cytokine that control the development of Th17 cells by interacting with IL-12Rβ1 and the IL-23 receptor. It is composed of two subunits, IL-23p19 and IL-23p40, linked by a disulfide bond, which influence cell differentiation, proliferation, migration, and apoptosis. Their crystal structures available in the Protein Data Bank (PDB) under accession codes P40:5MZV and P19:3D87 (Beyer et al., 2008; Bloch et al., 2018). The long for these subunits are 198 base pairs for p19 and 328 base pairs for p40. (figure 9, 10)

The three-dimensional crystal structure of P19 and P40 were downloaded from the protein data bank (Bank, n.d.) and processed using Schrödinger's Maestro Modelling Suite Molecular-Protein Preparation Wizard for drug screening (Madhavi Sastry et al., 2013). The preparation included removal of unnecessary chains and molecules from the 5MZV structure, e.g. IL-23R, Nanobody22E11, other sugar molecules that were not relevant to this study's objective. In the case of the P19 subunit in 3D87, the same procedure was used to remove unnecessary chains.

Subsequently, structures have been further refined, including the filling of missing loops and side chains using prime (Jacobson et al., 2004), the formation of disulfate bonds, and the addition of hydrogen atoms. The protein structures were then energy minimized and optimized using the OPLS3e force field (Harder et al., 2016). The protonation states of the proteins were adjusted for a pH of 7.4 using PROPKA, and any water molecules located beyond 5Å from hetero groups were removed, ensuring the proteins were optimally prepared for molecular docking (Harder et al., 2016).

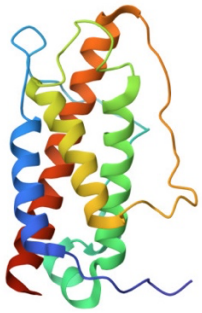

Figure 9. P19/Subunit Alpha of IL-23

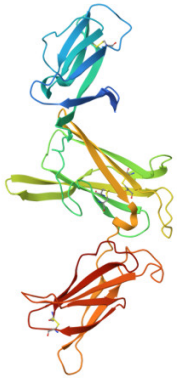

Figure 10. P40/Subunit Beta of IL-23

3.3 Ligand Preparation

The LigPrep module of the Maestro software was used to process compounds from two different small molecule libraries, the FDA and ChemBridge databases, in order to produce the 3D structures of each molecule (Chen & Foloppe, 2010). In this stage of preparation, the ionization states of the molecules at a pH range of 7.0 ±2.0 were predicted using the Epik tool (Shelley et al., 2007). This can lead to the formation of multiple stereoisomers because the molecules have chiral centers. As a result, each molecule could produce up to four stereoisomers and matching ionization states. During the preparation phase, the OPLS3e force field was used to guarantee an accurate representation of molecular properties (Roos et al., 2019).

3.4 Receptor Grid Generation

The critical first step to set up the ligand-protein docking job is receptor grid generation. In this process, a cubic box of specified dimensions, typically with each side measuring 20 Å, is created around the center of the predicted binding sites (active sites). This box helps to localize the interactions in order to calculate them later. Although the box is generally rigid, some degree of flexibility can be maintained by allowing certain bonds to rotate around the active site in order to facilitate a more dynamic interaction between ligand and receptor (Friesner et al., 2006; Zhang et al., 2020). The active site of

IL-23p19 and IL-23p40 has been defined according to the available data from literature review.

The receptor grid generation of IL-23p40 was generated based on an in-silico study aimed at identifying potent inhibitors for psoriasis, as detailed in the study by (Halim et al., 2020). The generating was built with a default measurement of 20 Å on all side and centroid around of a cluster of key residues of selected residues as critical for interaction: Leu56, Arg57, Glu58, Trp156, Leu160, Lys164. The (x, y, z) coordinates of the grid center are (-32.68, -6.03, -32.19). Where, the receptor grid generation of IL-23p19 was generated based on an in-silico study published in 2022 (Berniyanti et al., 2022). The (x, y, z) coordinates of the grid center are (34.784, 32.333, 30.075) and the dimension Å is (46.012, 72.949, 78.274).

3.5 Molecular Docking

A computational technique called "Virtual Screening" is used to sort through large libraries of small molecules and find the ones that are most likely to bind with a therapeutic target. For ligand-receptor interactions in our investigation, we used the Glide module of Schrödinger's Maestro Modelling Suite. Three different approaches—HTVS (high throughput virtual screening), SP (standard precision), and XP (extra precision)—are used usually by Glide docking to filter small molecules (Friesner et al., 2004). The complexity and accuracy of each approach varies. To ensure a balance between computational efficiency and accuracy in predicting binding modes and affinities between small molecules and IL-23 subunits, we implemented the Glide docking/ SP protocol using the default settings for our purposes (Giordano et al., 2022; Madhavaram et al., 2019).

To perform the SP docking protocol, we selected the SP mode with flexible ligand sampling by using Schrödinger's Maestro's-Glide option. In order to account for high energy states, we incorporated Epik state penalties (Shelley et al., 2007) and used the OPLS3 force field to refine the ligand in torsional space with respect to the receptor (Roos et al., 2019). Only the TOP 100 frames were prepared for post-docking minimization. The prepared-ligand and poses protein files were two essential files that were needed. The docking process was run four times in our study with the same default settings each time. To be more precise, we docked IL-23p19 with the FDA databases first, and then IL-23p19

with the ChemBridge database. We then went through the same procedure twice for IL-23p40: once using the FDA databases and once using the ChemBridge database.

3.6 Molecular Dynamic (MD) Simulation

Molecular Dynamics Simulation is a computational method uses to simulate the dynamic behavior of molecules by determining the forces acting on each atom in the system (Chemical bonds, atomic angles, rotation bonds and non-bonded forces). By simulating atoms' motion over time in accordance with Newton's laws of motion, this technique sheds light on the dynamic and structural characteristics of molecules in a variety of settings.

In accordance with our study, the top 100 molecules from each library and subunit, as determined by their docking score in the Glid/SP docking step were subjected to MD simulation using the Desmond software (Bowers et al., 2006). Explicit water molecules (TIP3P model) with a thickness of 10 Å from the protein edges were used in an orthorhombic simulation box (Jorgensen et al., 1983). 0.15 M NaCl was added to the system at PH 7.4 to neutralize it. The particle mesh Ewald method was used to handle long-range electrostatic interactions, with a 9.0 Å cut-off for both electrostatic and van der Waals interactions (Essmann et al., 1995). The system was simulated under an isothermal–isobaric ensemble (NPT) and used the Nose-Hoover thermostat and the Martyna-Tobias-Klein barostat to maintain a constant temperature (310 K) and pressure (1.01325 bar) (Evans & Holian, 1985; Martyna et al., 1992). In MD simulations, the OPLS3e force field was used to calculate the atomistic interactions. A total of 100 trajectory frames were gathered for each system at regular intervals. Using time steps of 2.0 femtoseconds for bonded interactions, 2.0 femtoseconds for near non-bonded interactions, and 6.0 femtoseconds for far non-bonded interactions, interaction integration was carried out using the RESPA integrator. Multiple simulations were conducted over three different timeframes, with each subsequent duration informed by the results of the previous MM/GBSA analysis: 1) a short duration of 1 nanosecond, 2) a moderate duration of 10 nanoseconds, and 3) a long duration of 100 nanoseconds.

3.7 Molecular Mechanics the Generalized Born Solvent Accessible Surface Area (MM/GBSA) Calculations.

Protein- ligand free energies were calculated after each MD simulation using Molecular mechanics generalized born solvent accessible surface area (MM/GBSA) calculation, which implemented in Prime module of Schrödinger's molecular modelling package. The MM/GBSA is calculated on a collection of a snapshot generated by the MD simulation in order to employ the trajectory frames and calculate the average of MM/GBSA. The VSGB 2.0 solvation model in Prime (Li et al., 2011) and the OPLS3e force field were used to simulate the interactions. The water system exterior was treated with a constant dielectric constant of 80 (Li et al., 2011). The mean and standard deviation were calculated as a final $\Delta G\ bind$ for each compound (Forouzesh & Mishra, 2021). The top 10 negative scores obtained from the 1ns-MM/GBSA calculation were selected for the subsequent 10 ns molecular dynamics (MD) simulation. Similarly, the top 5 negative scores from the 10ns-MM/GBSA results were chosen for the 100ns simulation. This stepwise approach ensured that only the most promising compounds, as determined by their free energy scores, were subjected to longer and more computationally intensive MD simulations.

3.8 Quantitative structure–activity relationship Model (QSAR Model) and METACORE™/METADRUG™

QSAR is a computational mathematical modeling method designed to predict the biological activates of a compound based on knowledge two dimensional (2D) and three dimensional (3D) chemical structures. To achieve this, QSAR modeling built on the basis of training sets with known biological activity to help prioritize a large number of other unknown chemicals in order to reduce the candidate's numbers that need to be tested in vivo (Kwon et al., 2019; Vilar & Costanzi, 2012).

Where the METACORE™/METADRUG™ is a tool developed by Clarivate Analytics to study how small molecules affect the human body through the use of various trained QSAR models that predict pharmacokinetic, toxicological, and therapeutic action. This platform has 26 distinct toxicity models and QSAR models for 25 common disorders

(Ekins et al., 2006). In the aspect of our research and in order to anticipate therapeutic activity values, the four hit small inhibitors that were selected from 1ns, 10ns, and 100ns MD simulation with their MM/GBSA were converted to SDF format and uploaded to the METACORE™/METADRUG™ database. Values were normalized to be between 0 and 1, with values greater than 0.5 can be a sign of therapeutic promise.

Chapter 4: Result

4.1 Result of IL-23p19 subunit and FDA database:

In the first part, we will introduce the result of docking the prepared p19 protein with ligands obtained from the FDA databases. Following with the result of three rounds of molecular dynamics (MD) simulation and MMGBSA. MM/GBSA analysis was performed after a short simulation (1 ns) in the first round. Then, selecting the hit molecules from the MM/GBSA calculations and undergoing an additional round of molecular dynamics simulation (10ns) and MM/GBSA. The molecules that were identified as hits from the second MM/GBSA results underwent further long MD simulation (100ns) and MM/GBSA analysis. These results are displayed below.

4.1.1 Docking Result.

Docking with IL-23p19 was applied to all FDA small molecules using the Glid/SP virtual screening workflow tool in Maestro. As shown in Table1, the top 100 hit molecules resulted from the docking were listed to use in the MD simulation analysis based on their lowest docking scores, which ranged from -8.548 kcal/mol to -6.182 kcal/mol. Table 1 included the candidate's names, their docking score and glide ligand (LE) efficiency scores. The last is a matric software to evaluate the efficiency of the ligand in term of its binding affinity relative to its size and complexity (Kenny, 2019).

Table 1.

Top 100 Molecules of FDA Library with P19 and Their Docking Scores.

Title	Docking score kcal/mol	Glide ligand efficiency kcal/mol
Iotrolan	-8.548	-0.128
Iodixanol	-7.953	-0.128
Berotralstat	-7.771	-0.19
Posaconazole	-7.749	-0.152

Iotrolan	-7.694	-0.115
Iotrolan	-7.601	-0.113
Cobicistat	-7.512	-0.139
Dequalinium	-7.453	-0.219
Iotrolan	-7.426	-0.111
Light green SF yellowish	-7.349	-0.144
Vilanterol	-7.289	-0.228
Revefenacin	-7.222	-0.164
Chlorthalidone	-7.207	-0.328
Salmeterol	-7.204	-0.24
Macimorelin	-7.177	-0.205
Salmeterol	-7.148	-0.238
Dyphylline	-7.134	-0.396
Digoxin	-7.133	-0.13
Fenoterol	-7.111	-0.323
Acarbose	-7.094	-0.161
Fenoterol	-7.021	-0.319
Isavuconazonium	-7.015	-0.138
Carfilzomib	-6.997	-0.135
Fenoterol	-6.991	-0.318
Iobitridol	-6.99	-0.2
Tenapanor	-6.948	-0.094
Iopromide	-6.946	-0.217
Brexpiprazole	-6.922	-0.223
Eluxadoline	-6.908	-0.164
Indoramin	-6.900	-0.265
Theophylline	-6.869	-0.528
Ioxilan	-6.851	-0.214
Indocyanine green	-6.844	-0.129
Isavuconazonium	-6.837	-0.134
Cabozantinib	-6.812	-0.184
Venetoclax	-6.801	-0.111
Digitoxin	-6.784	-0.126

Nebivolol	-6.769	-0.233
Iodixanol	-6.757	-0.109
Remdesivir	-6.739	-0.16
Hyaluronic acid	-6.711	-0.127
Iopromide	-6.689	-0.209
Carbetocin	-6.684	-0.097
Nilotinib	-6.626	-0.17
Tazemetostat	-6.617	-0.158
Iopromide	-6.614	-0.207
Lypressin	-6.608	-0.091
Iobitridol	-6.596	-0.188
Aprepitant	-6.578	-0.178
Pentostatin	-6.578	-0.346
Esculin	-6.577	-0.274
Temozolomide	-6.56	-0.469
Dabigatran etexilate	-6.527	-0.142
Oxamniquine	-6.51	-0.325
Pralsetinib	-6.506	-0.167
Frovatriptan	-6.500	-0.361
Terbutaline	-6.495	-0.406
Propylthiouracil	-6.493	-0.59
Ioxilan	-6.478	-0.202
Rutin	-6.472	-0.151
Hydroxystilbamidine	-6.472	-0.308
Idebenone	-6.472	-0.249
Lopinavir	-6.468	-0.141
Vibegron	-6.455	-0.196
Sapropterin	-6.453	-0.38
Lapatinib	-6.442	-0.161
Pasireotide	-6.416	-0.083
Orciprenaline	-6.414	-0.428
Arbutin	-6.391	-0.336
Tenapanor	-6.389	-0.086

Indocyanine green acid form	-6.388	-0.121
Dyphylline	-6.388	-0.355
Alcloxa	-6.388	-0.581
Atogepant	-6.385	-0.148
Dantrolene	-6.379	-0.277
Inosine pranobex	-6.379	-0.336
Iohexol	-6.378	-0.188
Phenylephrine	-6.351	-0.529
Metaraminol	-6.346	-0.529
Glutethimide	-6.333	-0.396
Phenylpropanolamine	-6.316	-0.574
Procaine benzylpenicillin	-6.316	-0.275
Iodixanol	-6.300	-0.102
Amikacin	-6.295	-0.157
Ergotamine	-6.282	-0.146
1-Palmitoyl-2-oleoyl-sn-glycero-3-(phospho-rac-(1-glycerol))	-6.275	-0.123
Protokylol	-6.252	-0.260
Hexamidine	-6.251	-0.240
Ripretinib	-6.246	-0.189
Iomeprol	-6.244	-0.201
Nebivolol	-6.239	-0.215
Mizolastine	-6.239	-0.195
Tezacaftor	-6.237	-0.169
Ioxilan	-6.236	-0.195
Panobinostat	-6.232	-0.240
Benperidol	-6.202	-0.222
Dasatinib	-6.202	-0.188
Fenoterol	-6.198	-0.282
Revefenacin	-6.195	-0.141
Raltitrexed	-6.184	-0.193

4.1.2 Molecular Dynamic (MD) simulation and MM/GBSA for (1ns, 10ns and 100ns). For the top 100 molecules found in the docking with the lowest docking scores, molecular dynamics (MD) simulations were run for 1 ns, 10 ns, and 100 ns, collecting 100 frames for each simulation. One hundred protein-ligand complex structures were taken from the trajectory files after the simulations were finished. All structures also had MM/GBSA calculations, and average values over all time periods were determined. Using a threshold value of -93.7 kcal/mol for 1ns MM/GBSA averages, a total of 4 molecules were identified in the 100ns MM/GBSA with values below the threshold. As listed in Table 2, the name hit candidates with their docking scores and MM/GBSA average scores over the three different time frames. Also, the binding pocket and surface ligand-protein interactions were illustrated in Figures (11-14) respectively.

Table 2.

Top Hit Molecules of FDA Library with p19 and Their MM/GBSA Scores.

Protein-Ligand complex	**Docking score (kcal/mol)**	**1ns MD-MM/GBSA (kcal/mol)**	**10ns MD-MM/GBSA (kcal/mol)**	**100ns MD-MM/GBSA (kcal/mol)**
Cobicistat	-7.512	-97.3281	-85.2905	-72.9979
Indocyanine green acid	-6.388	-97.8199	-97.8902	-97.2691
Lopinavir	-6.468	-93.7605	-94.9027	-86.1315
Tenapanor	-6.389	-98.2585	-86.9549	-101.6643

The following figures (11-14) represent the binding pocket and the 2D interaction map for the four hit molecules:

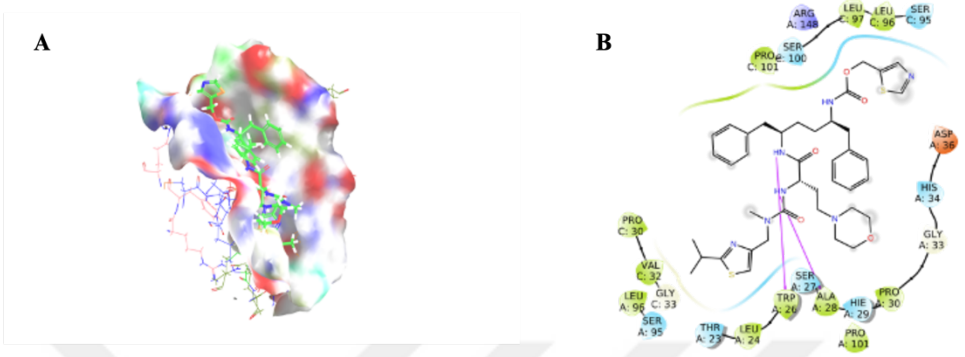

Figure 11. **A** Represent P19/ Cobicistat Binding Pocket. Where **B** Represent 2D Interaction Map of P19/ Cobicistat.

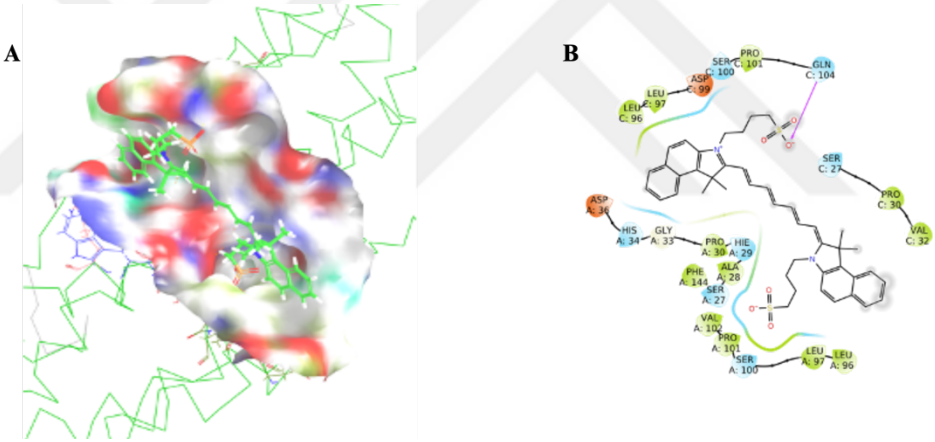

Figure 12. **A** Represent P19/ Indocyanine_gGeen_Acid Binding Pocket. Where **B** Represent 2D Interaction Map of P19/ Indocyanine_Green_Acid.

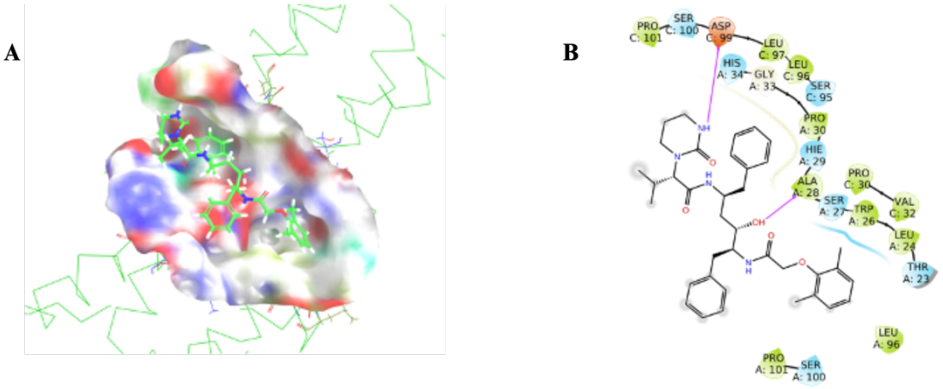

Figure 13. **A** Represent the P19/Lopinavir Binding Pocket. Where **B** Represent 2D Interaction Map of P19/ Lopinavir.

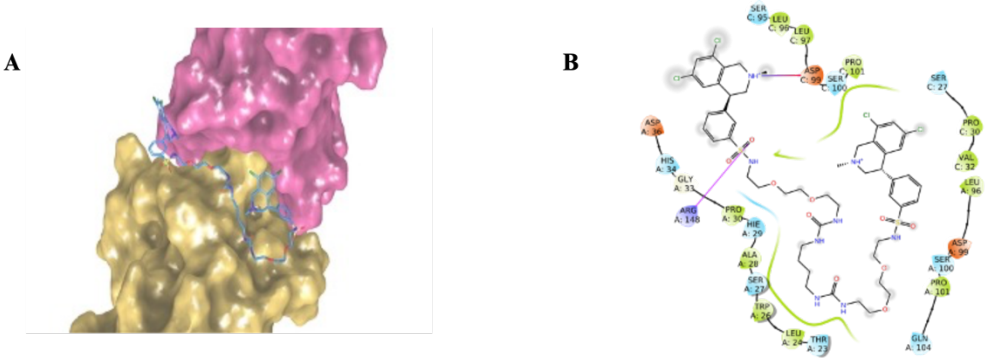

Figure 14. **A** Represent the P19/Tenapanor Binding Pocket. Where **B** Represent 2D Interaction Map of P19/Tenapanor.

The purpose of the results presented in Figures 11-14 and Table 2 were to investigate the protein-ligand interaction and the behavior of the ligands and their interactions over different simulation times. The result of Cobicistat which has the lowest docking score indicate that its MM/GBSA average significantly increased, its MM/GBSA was -97.3281kcal/mol in 1ns simulation, however, it increased to -72.9979 kcal/mol by increasing the simulation time to 100ns. This change in MM/GBSA calculations suggested weaker protein-ligand interactions and less favorable binding affinity when the simulation time increased which leads to unstable interactions within the protein and ligand in the binding site. Conversely, Tenapanor showed decreasing in the MM/GBSA when the simulation time had increased, where it has -98.2585 kcal/mol on 1ns and became -101.6643 kcal/mol on 100ns, indicating more favorable interactions and potentially stronger binding affinity comparing to other candidates. Detailed analysis of the molecular dynamic simulation of Tenapanor was conducted and the findings are illustrated through interaction diagrams and histograms (Figure15)

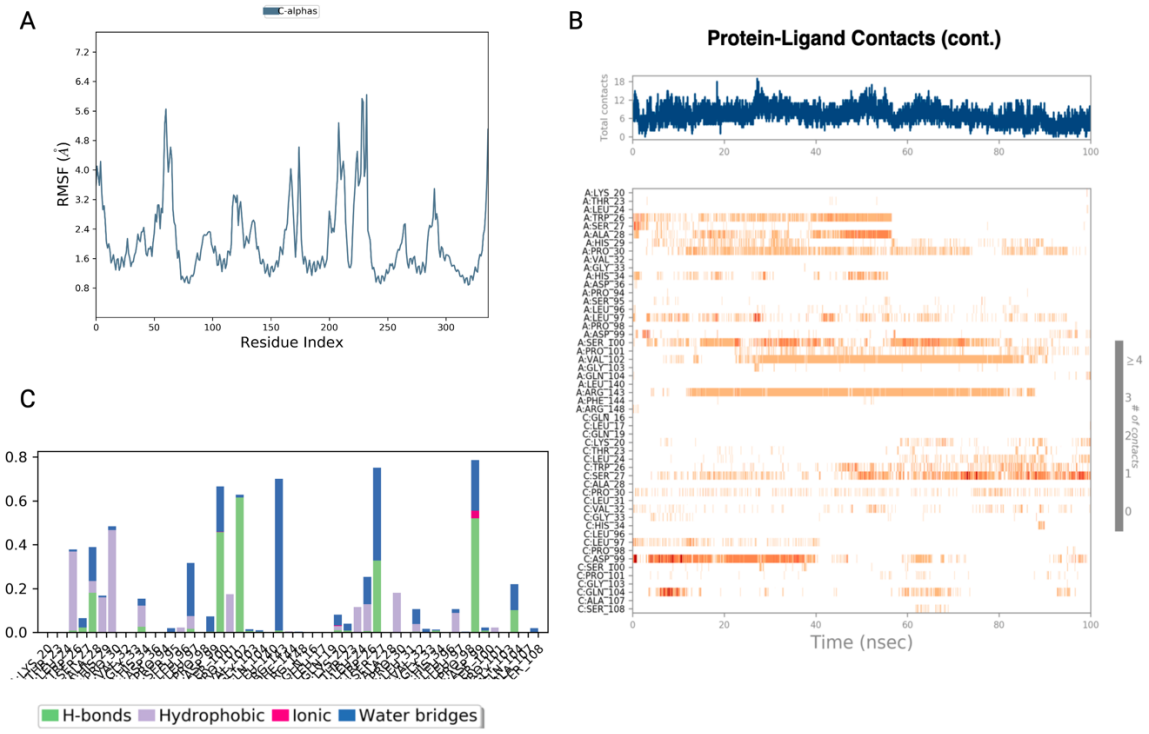

Figure 15. **A** Represent the RMSF Calculation, **B** Represent the Interaction and Contacts Observed During the Simulation, and **C** Show the Dynamic Changes in Contacts During 100ns MD Simulation.

Figure 15 illustrates the interaction between P19 and Tenapanor, where it identified as the most promising hit within the P19/FDA database. In Figure A, the Root Mean Square Fluctuation (RMSF) represents the local fluctuations of the protein chain throughout the simulation. Peaks in the graph indicate regions of the protein that exhibit significant fluctuations during the simulation, typically observed in the N- and C-terminal regions as well as in loop regions. Figure B illustrates the interactions and contacts observed during the simulation. Notably, ASP99 exhibits substantial interaction during the initial 40ns, while SER27 demonstrates significant interaction towards the simulation's end (60-100ns), and ARG143 displays interaction during the midsection of the simulation (15-85ns). Figure C highlights the dynamic changes in contacts between Tenapanor and P19 over the simulation. During the 100ns simulation time, residues VAL102, SER100, and ASP99 are

observed to form hydrogen bonds with the ligand, maintaining stability throughout the simulation. Notably, VAL102 and ASP99 also engage in ionic and water bridge bonds. These hydrogen bonds play a crucial role in influencing drug specificity, metabolism, and absorption. It also demonstrates favorable hydrophobic interactions with TRP 26, PRO 30, and PRO 101.

4.2 Result of IL-23p40 subunit with FDA database:

The next stage of the in silico investigation proceeded according to the previously mentioned protocol, which included docking the prepared p40 protein with ligands from the FDA databases, followed by three rounds of molecular dynamics simulations and MM/GBSA (1ns, 10ns, and 100ns). The following is an outline of the results.

4.2.1 Docking Result. Docking with IL-23p40 was applied to all FDA small molecules using the SP Glide in Maestro. As shown in Table3, the top 100 hit molecules from this screening were chosen for additional MD simulation analysis based on their lowest docking scores, which ranged from -7.686 kcal/mol to -4.999 kcal/mol.

Table 3.

Top 100 Molecules of FDA Library with P40 and Their Docking Scores.

Title	Docking score kcal/mol	Glide ligand efficiency kcal/mol
Capreomycin	-7.686	-0.164
Iotrolan	-7.465	-0.111
Tenapanor	-7.248	-0.098
Isavuconazonium	-7.215	-0.141
Tenapanor	-6.882	-0.093
Colistin	-6.741	-0.083
Hydroxyethyl cellulose	-6.596	-0.120
Iobitridol	-6.217	-0.178
Netilmicin	-6.157	-0.187
Pixantrone	-6.084	-0.253

Berotralstat	-6.08	-0.148
Iotrolan	-5.981	-0.089
Ribostamycin	-5.972	-0.193
Domperidone	-5.971	-0.199
Saquinavir	-5.968	-0.122
Dabigatran etexilate	-5.947	-0.129
Ritonavir	-5.920	-0.118
NADH	-5.824	-0.132
Tepotinib	-5.812	-0.157
Amikacin	-5.803	-0.145
Ioxilan	-5.759	-0.18
Plazomicin	-5.747	-0.14
Xamoterol	-5.729	-0.239
Isavuconazonium	-5.700	-0.112
Iohexol	-5.675	-0.167
Haloperidol	-5.674	-0.218
Tenapanor	-5.656	-0.076
Ioversol	-5.655	-0.171
Lusutrombopag	-5.638	-0.145
Paromomycin	-5.628	-0.134
Revefenacin	-5.599	-0.127
Ioversol	-5.589	-0.169
Hesperidin	-5.538	-0.129
Entrectinib	-5.525	-0.135
Atracurium besylate	-5.484	-0.082
Allantoin	-5.474	-0.498
Alcloxa	-5.470	-0.497
Dextroamphetamine	-5.460	-0.546
Iobitridol	-5.454	-0.156
Iodixanol	-5.448	-0.088
Difelikefalin	-5.444	-0.111
Flavin adenine dinucleotide	-5.442	-0.103
Niraparib	-5.419	-0.226

Mitoxantrone	-5.410	-0.169
Vinorelbine	-5.400	-0.095
Naratriptan	-5.391	-0.234
Saquinavir	-5.377	-0.110
Levonordefrin	-5.368	-0.413
Iobitridol	-5.367	-0.153
Dihydroergocristine	-5.367	-0.119
1-Palmitoyl-2-oleoyl-sn-glycero-3-(phospho-rac-(1-glycerol))	-5.348	-0.105
Maraviroc	-5.348	-0.145
Phenylpropanolamine	-5.347	-0.486
Erdafitinib	-5.318	-0.161
Levetiracetam	-5.293	-0.441
Bisoxatin	-5.281	-0.211
Trimethaphan	-5.279	-0.203
Lopinavir	-5.279	-0.115
Eletriptan	-5.278	-0.195
Dipivefrin	-5.276	-0.211
Phentermine	-5.271	-0.479
Natamycin	-5.264	-0.112
Kanamycin	-5.258	-0.159
Migalastat	-5.256	-0.478
Propafenone	-5.253	-0.210
Framycetin	-5.246	-0.125
Ceftolozane	-5.245	-0.117
Aclidinium	-5.228	-0.158
Plerixafor	-5.223	-0.145
Xamoterol	-5.218	-0.217
Cobimetinib	-5.208	-0.174
Mefloquine	-5.182	-0.199
Isoxsuprine	-5.164	-0.235
Netarsudil	-5.157	-0.152
Ioversol	-5.153	-0.156

Estetrol	-5.145	-0.234
Piracetam	-5.143	-0.514
Estradiol	-5.141	-0.257
Methoxamine	-5.132	-0.342
Cabozantinib	-5.130	-0.139
Mazindol	-5.129	-0.256
Maralixibat	-5.127	-0.107
Tetryzoline	-5.109	-0.341
Mirabegron	-5.105	-0.182
Deferoxamine	-5.097	-0.131
Iopromide	-5.097	-0.159
Propylthiouracil	-5.094	-0.463
Temozolomide	-5.084	-0.363
Silodosin	-5.079	-0.145
Avacopan	-5.074	-0.121
Entecavir	-5.062	-0.253
Micronomicin	-5.047	-0.158
Carvedilol	-5.046	-0.168
Phenylethyl resorcinol	-5.045	-0.315
Benperidol	-5.042	-0.180
Halofantrine	-5.027	-0.152
Hydroxyamphetamine	-5.016	-0.456
Ephedrine	-5.009	-0.417
Methscopolamine bromide	-5.003	-0.218
Promethazine	-4.999	-0.250

4.2.2 **Molecular Dynamic (MD) simulation and MMGBSA.** For the top 100 molecules found in the docking job, molecular dynamics simulations were run for 1 ns, 10 ns, and 100 ns, collecting 100 frames for each simulation. One hundred protein-ligand complex structures were taken from the trajectory files after the simulations were completed. All structures also had MM/GBSA calculations, and average values over all time periods were determined. As listed in Table 4, the hit candidates that emerged from the three simulation rounds are Piracetam, Propylthiouracil, Temozolomide, Hydroxyamphetamine, and Ephedrine.

Table 4.

Top Hit Molecules of FDA Library with P40 and Their MM/GBSA Scores.

Protein-Ligand complex	**Docking score (kcal/mol)**	**1ns MD-MM/GBSA (kcal/mol)**	**10ns MD-MM/GBSA (kcal/mol)**	**100ns MD-MM/GBSA (kcal/mol)**
Piracetam	-5.143	-23.0265	-27.1528	-28.8437
Propylthiouracil	-5.094	-25.3836	-28.0667	-26.9661
Temozolomide	-5.084	-22.6925	-28.2721	-30.6036
Hydroxyamphetamine	-5.016	-24.9911	-30.1275	-18.0575
Ephedrine	-5.009	-19.9083	-31.0444	-24.5224

The purpose of the results presented in table 4 is to investigate the behavior of the ligands over different simulations time. The result of Temozolomide which has the lowest MM/GBSA score showed decreasing in the MM/GBSA scores when the simulation time had increased, where it has -22.6925 kcal/mol on 1ns and became -30.6036 kcal/mol on 100ns, indicating more favorable interactions and potentially stronger binding affinity comparing to other candidates. However, the trajectory file of Temozolomide suggests a different outcome. The simulation trajectory did not generate the expected files, such as protein and ligand RMSF, protein and ligand contacts, and other relevant data in order to observe the behavior and interaction between the receptor and ligand. This could be due to

the ligand escaping from the binding pocket, as observed when loading the trajectory in the Maestro workspace. The ligand was stable within the binding pocket in the beginning of simulation; however, it started moving out of the binding pocket at 50ns and eventually escaped entirely. As shown in Figure 16 (A, B, C, and D) multiple snapshots were taken over different timeframes from 1 to 100 ns.

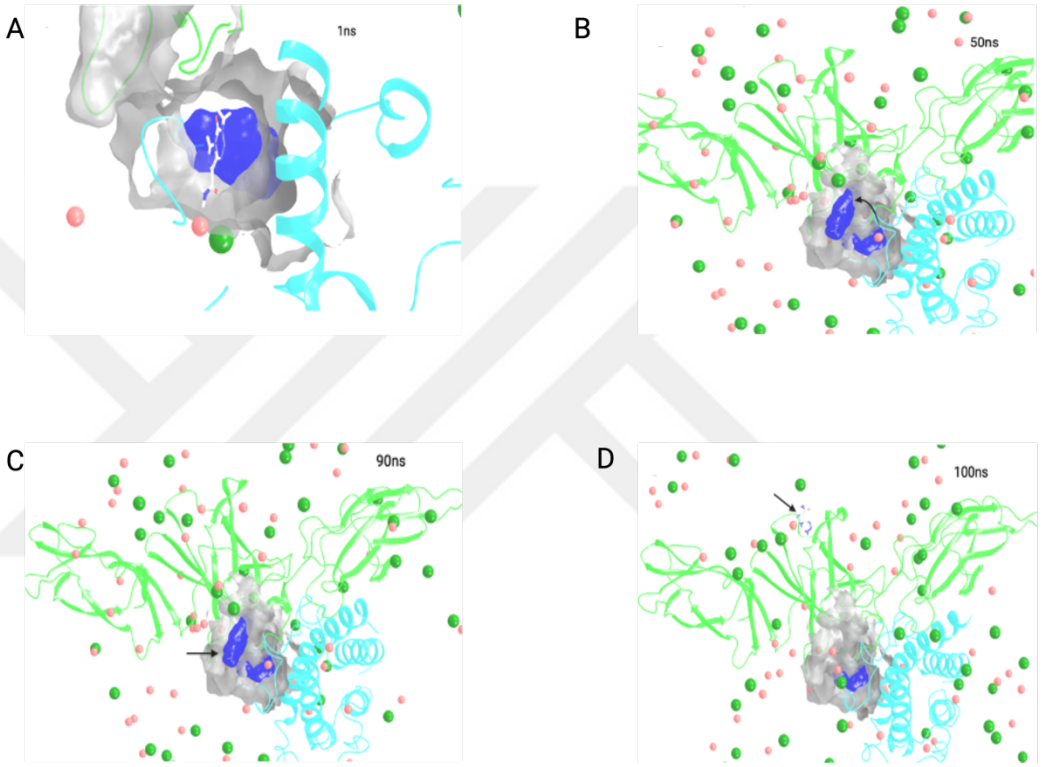

Figure 16. **A)** At 1ns, the Ligand in the Binding Pocket, **B)** At 50ns, the Ligand Moved to Another Site (the Direction of Arrow Represent the Moving of Ligand from One Site to Another), **C)** 90ns (the Direction of Arrow Represent the Location of Ligand) and **D)** At 100.

The following figures (17-21) represent the binding pocket and the 2D interaction map for the five hit molecules:

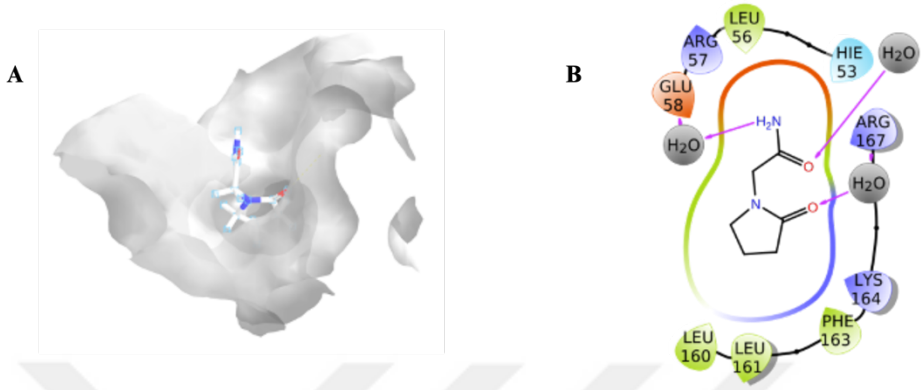

Figure 17. **A** Represent the P40/ Piracetam Binding Pocket. Where **B** Represent 2D Interaction Map of P40/ Piracetam.

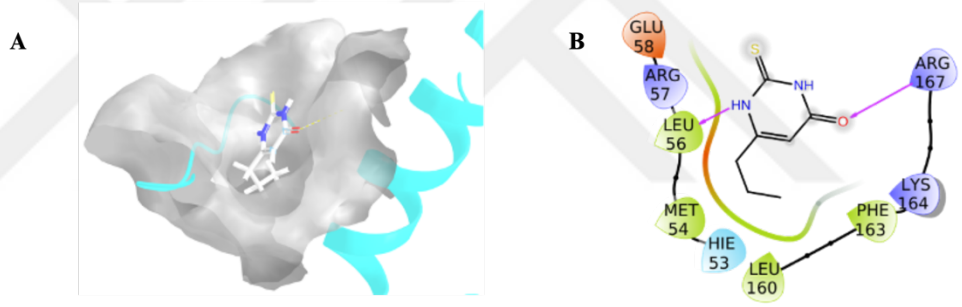

Figure 18. **A** Represent the P40/ Propylthiouracil Binding Pocket. Where **B** Represent 2D Interaction Map of P40/ Propylthiouracil.

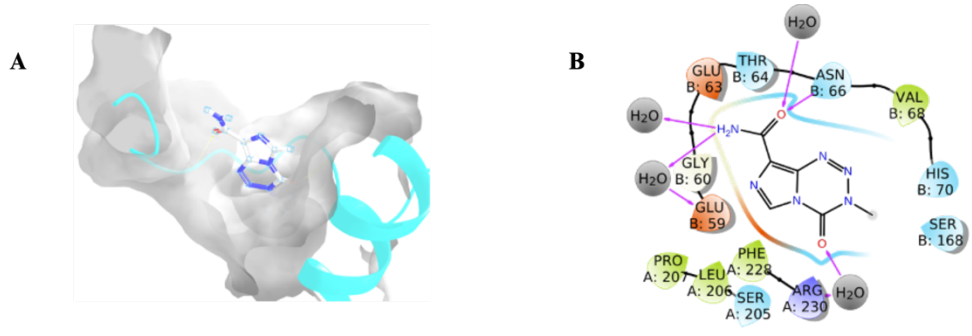

Figure 19. **A** Represent the P40/ Temozolomide Binding Pocket. Where **B** Represent 2D Interaction Map of P40/ Temozolomide.

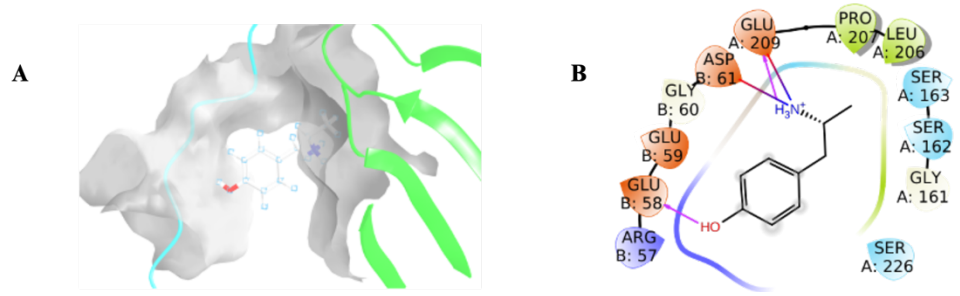

Figure 20. **A** Represent the P40/Hydroxyamphetamine Binding Pocket. Where **B** Represent 2D Interaction Map of P40/ Hydroxyamphetamine.

Figure 21. **A** Represent the P40/ Ephedrine Binding Pocket. Where **B** Represent 2D Interaction Map of P40/ Ephedrine.

4.3 Result of IL-23p19 subunit with ChemBridge database:

The next stage of the in silico investigation proceeded according to the previously mentioned protocol, which included docking the prepared p19 protein with ligands from the ChemBridge library, followed by three rounds of molecular dynamics simulations and MM/GBSA (1ns, 10ns, and 100ns). The following is an outline of the methodologies' results.

4.3.1 **Docking Result.** Docking with IL-23p19 was applied to all ChemBridge small molecules using the SP Glide tool in Maestro. As shown in Table 5, the top 100 hit molecules from this screening were chosen for additional MD simulation analysis based on their lowest docking scores, which ranged from -9.634 kcal/mol to -7.524 kcal/mol.

Table 5.

Top 100 Molecules of ChemB Library with P19 and Their Docking Scores.

ChEMBL ID	Docking score kcal/mol	Glide ligand efficiency kcal/mol
899269	-9.634	-0.357
897840	-8.855	-0.354
1153899	-8.823	-0.315
1520093	-8.756	-0.172
1234731	-8.740	-0.301
1205899	-8.732	-0.323
925688	-8.729	-0.349
1044248	-8.658	-0.361
894626	-8.628	-0.332
1128603	-8.605	-0.319
738516	-8.573	-0.357
1058789	-8.572	-0.343
1234731	-8.564	-0.295
721889	-8.480	-0.314
1052550	-8.473	-0.353
747048	-8.472	-0.368
1103916	-8.466	-0.314
1146095	-8.463	-0.353
763496	-8.448	-0.338
960402	-8.439	-0.291
634396	-8.425	-0.201
739102	-8.422	-0.272

432299	-8.404	-0.247
1061731	-8.395	-0.350
979287	-8.394	-0.323
425619	-8.393	-0.254
725889	-8.379	-0.270
1061728	-8.350	-0.334
866019	-8.342	-0.379
752854	-8.324	-0.308
1021358	-8.317	-0.308
858624	-8.315	-0.308
1044248	-8.310	-0.346
1242047	-8.310	-0.160
960402	-8.309	-0.287
1064144	-8.296	-0.307
856356	-8.292	-0.377
741885	-8.285	-0.193
886531	-8.253	-0.330
1002019	-8.240	-0.358
685031	-8.238	-0.250
1455283	-8.229	-0.158
878646	-8.215	-0.329
1362142	-8.212	-0.179
1269657	-8.198	-0.293
515396	-8.197	-0.304
1145193	-8.196	-0.293
1235733	-8.183	-0.315
1278162	-8.155	-0.281
574083	-8.146	-0.302
728221	-8.136	-0.262
1066877	-8.130	-0.370
682722	-8.129	-0.301
1004107	-8.129	-0.301
1567489	-8.123	-0.246

689304	-8.121	-0.301
1343895	-8.111	-0.166
819499	-8.103	-0.312
1025036	-8.089	-0.289
688875	-8.071	-0.269
323377	-8.070	-0.288
806857	-8.069	-0.299
1053187	-8.069	-0.299
81684	-8.067	-0.278
1520763	-8.063	-0.218
386174	-8.056	-0.237
1291895	-8.050	-0.288
610083	-8.047	-0.298
1072236	-8.042	-0.322
1330349	-8.040	-0.146
660742	-8.035	-0.268
739102	-8.031	-0.259
1519294	-8.029	-0.335
1074486	-8.028	-0.401
776875	-8.018	-0.229
1292559	-8.018	-0.297
271538	-8.017	-0.259
305219	-8.012	-0.276
267155	-8.007	-0.276
1345219	-8.007	-0.163
650923	-8.000	-0.320
866500	-7.999	-0.296
1130107	-7.981	-0.333
1066660	-7.979	-0.307
1345590	-7.978	-0.160
664843	-7.977	-0.285
1528828	-7.973	-0.221
1153682	-7.968	-0.306

1181793	-7.963	-0.295
238054	-7.959	-0.362
881681	-7.949	-0.306
581716	-7.946	-0.274
660252	-7.942	-0.274
750793	-7.942	-0.318
360118	-7.940	-0.194
605085	-7.940	-0.234
464326	-7.940	-0.467
24925	-7.939	-0.305
658165	-7.932	-0.256
1019879	-7.926	-0.294
1548397	-7.526	-0.243
1336950	-7.525	-0.164
1364308	-7.524	-0.148
575349	-7.524	-0.269

4.3.1 Molecular Dynamic (MD) simulation and MMGBSA. For the top 100 molecules found in the docking job, molecular dynamics simulations were run for 1 ns, 10 ns, and 100 ns, collecting 100 frames for each simulation. One hundred protein-ligand complex structures were taken from the trajectory files after the simulations were finished. All structures also had MM/GBSA calculations, and average values over all time periods were determined. The hit candidates that emerged from the three simulation rounds are listed in Table 6 with their ChEMBL IDs, docking scores, and MM/GBSA scores.

Table 6.

Top Hit Molecules of ChemB Library with p19 and Their MM/GBSA Scores.

Protein-Ligand complex	Docking score (kcal/mol)	1ns MD-MM/GBSA (kcal/mol)	10ns MD-MM/GBSA (kcal/mol)	100ns MD-MM/GBSA (kcal/mol)
1520093	-8.756	-93.6293	-91.0008	-87.6561
1242047	-8.31	-104.7021	-92.9136	-89.8665
1345219	-8.007	-99.7399	-88.7356	-81.0639
360118	-7.94	-93.2946	-92.8681	-91.0027
1336950	-7.525	-83.3826	-84.6344	-82.1754

The following Figures (22-26) represent the binding pocket and the 2D interaction map for the five hit molecules.

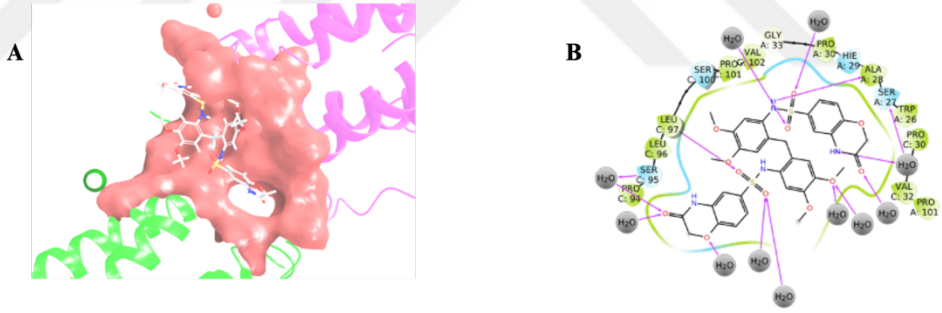

Figure 22. **A** Represent the P19/ 1520093 Binding Pocket. Where **B** Represent 2D Interaction Map of P19/ 1520093.

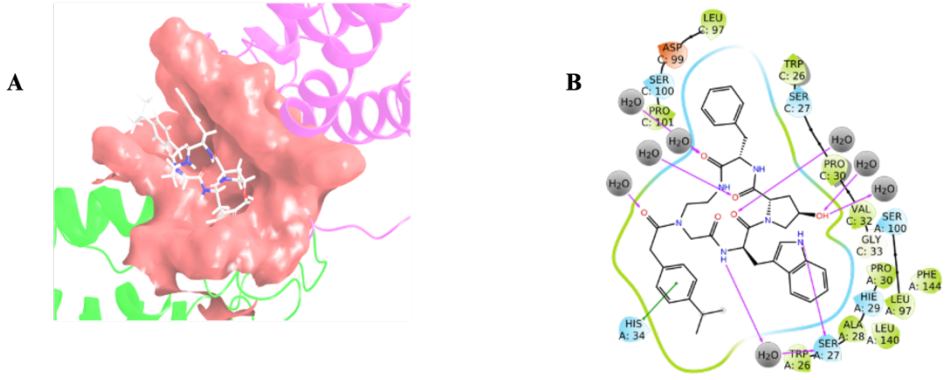

Figure 23. **A** Represent the P19/ 1242047 Binding Pocket. Where **B** Represent 2D Interaction Map of P19/ 1242047.

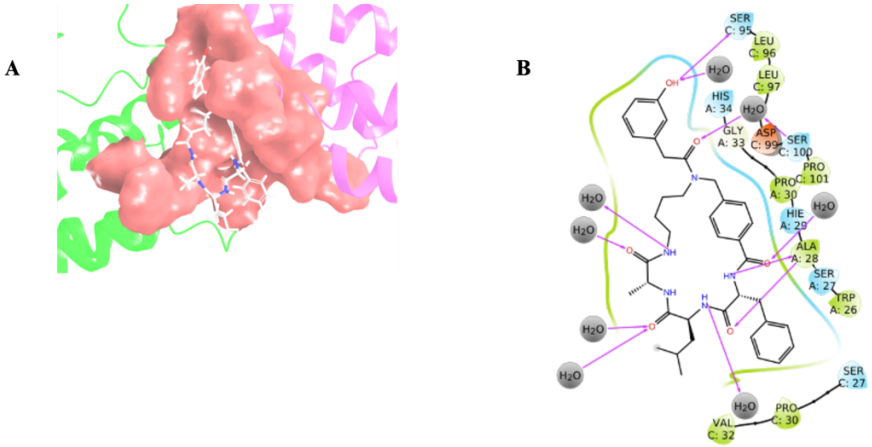

Figure 24. **A** Represent the P19/ 1345219 Binding Pocket. Where **B** Represent 2D Interaction Map of P19/ 1345219.

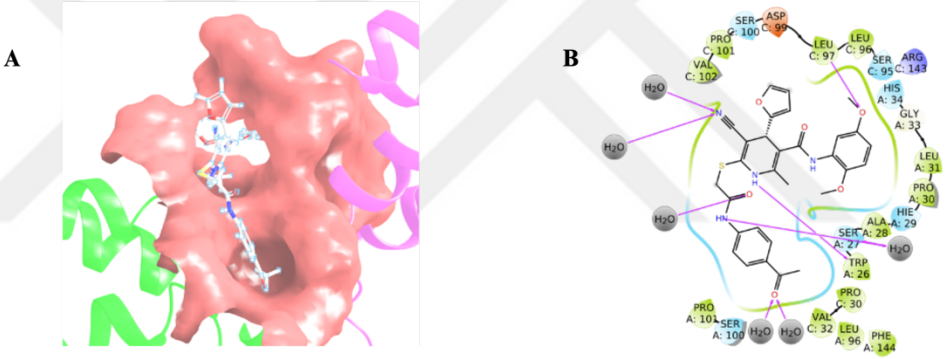

Figure 25. **A** Represent the P19/ 360118 Binding Pocket. Where **B** Represent 2D Interaction Map of P19/ 360118.

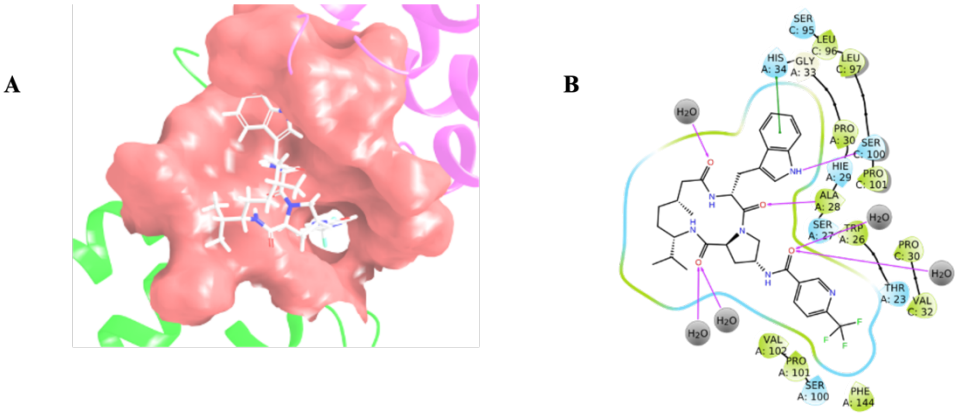

Figure 26. **A** Represent the P19/ 1336950 Binding Pocket. Where **B** Represent 2D Interaction Map of P19/ 1336950.

The purpose of the results presented in table 6 and figures (22-26) are to investigate the behavior of the ligands with IL-23p19 subunit over different MD simulation's time with calculating the MM/GBSA in each step. The result of the ChEMBL ID 360118 which has the lowest MM/GBSA score in 100ns MD simulation, showed increasing in the MM/GBSA when the simulation time had increased. Which means reaching -93.2946 kcal/mol on 1ns and increased to -91.0027 kcal/mol on 100ns, indicating decreasing in the binding affinity and the stability of interaction between the ligand and protein over different time of the MD simulation. However, in order to understand the behavior of the ligand-protein interaction during the 100 simulations, follow the following figure 27.

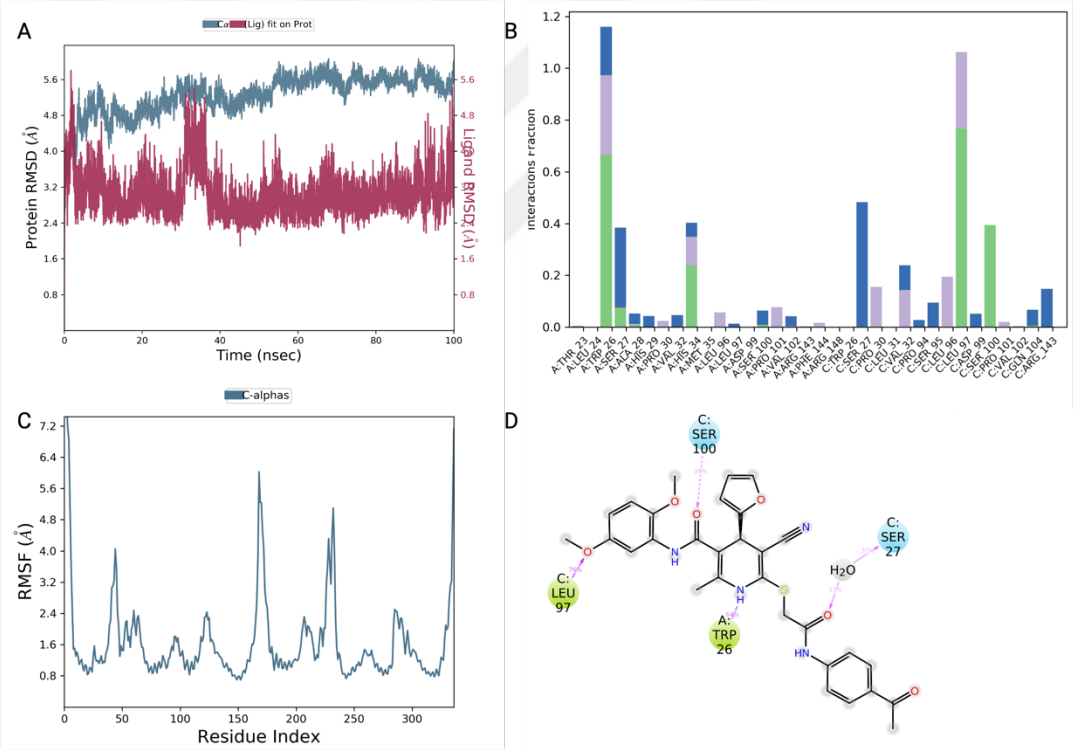

Figure 27. **A** Represent the RMSD, **B** Represent the Protein-Ligand Contacts, **C** Represent the RMSF, and **D** Represent the Ligand-Protein Contacts.

(Green, purple, and blue colours represent the H-bond, hydrophobic interaction, and water bridge respectively).

(A) represents the Protein-ligand RMS deviation, measuring the average change in displacement of selected atoms. The changes in protein RMS deviation (left Y-axis) are reaching above 4Å, indicating large conformational changes in the protein during the simulation. However, the simulation stabilizes around 4.8Å to 5.8Å for most of the time, suggesting the system equilibrated well. In contrast, the ligand RMS deviation (right Y-axis) is smaller, showing that the ligand remained almost stable and stayed within the binding site of 2.4Å and 3.5Å throughout the simulation. However, the values of RMSD jumps drastically at 30ns until 35ns where it reaches 4.8Å. (B) depicts the protein-ligand contacts, monitoring their interaction throughout the simulation according to four types of bonds: Hydrogen bonds, Hydrophobic interactions, Ionic bonds, and Water bridges. The histogram shows that hydrogen bonds are formed with TRP26, HIS34, and LEU97, which are crucial for ligand binding. Hydrophobic interactions are also observed in the same residues at frequencies of 90%, 60%, and 80% of the simulation time, respectively. Additionally, favourable water bridges are demonstrated in residues SER27 in both subunits A and C. (C) illustrates the RMS fluctuation to characterize local changes in the protein chain, where peaks indicate areas with the highest fluctuations at different times during the simulation. Two significant fluctuations are observed, ranging from 2.4Å to 7.2Å, in residues between 150-180 and 230-250. The schematic figure (D) represents the ligand-protein contacts during the first 10ns of the simulation. As shown, LEU97 makes hydrophobic interactions with the ligand's oxygen, TRP26 interacts with N-H residues, and SER27 forms water bridges.

4.4 Result of IL-23p40 subunit with ChemBridge database:

The last stage of the in silico investigation proceeded according to the previously mentioned protocol, which included docking the prepared p40 protein with ligands from the Chembl databases, followed by three rounds of molecular dynamics simulations and MM/GBSA (1ns, 10ns, and 100ns). The following is an outline of these methodologies' results.

4.4.1 Docking Result. Docking with IL-23p40 was applied to all Chembl small molecules using the SP virtual screening workflow tool in Maestro. As shown in Table6, the top 100 hit molecules from this screening were chosen for additional MD simulation analysis based on their lowest docking scores, which ranged from -8.102 kcal/mol to -6.663 kcal/mol.

Table 7.

Top 100 Molecules of ChamB Library with P40 and Their Docking Scores.

Title	Docking score kcal/mol	Glide ligand efficiency kcal/mol
822104	-8.102	-0.426
1361747	-7.763	-0.134
702526	-7.750	-0.258
1348439	-7.652	-0.128
1362994	-7.600	-0.262
1371400	-7.548	-0.343
404030	-7.347	-0.262
777870	-7.331	-0.253
1241747	-7.312	-0.141
1431691	-7.251	-0.161
590633	-7.212	-0.288
1358033	-7.184	-0.248
740121	-7.180	-0.266
1051162	-7.162	-0.286
1401080	-7.148	-0.132
1354119	-7.115	-0.323
771191	-7.102	-0.263
947276	-7.080	-0.262
996116	-7.066	-0.283
686069	-7.036	-0.251
1155486	-7.013	-0.319
731087	-7.011	-0.226
1331879	-7.002	-0.304

992235	-7.000	-0.241
705321	-6.980	-0.205
1458273	-6.978	-0.142
950701	-6.974	-0.349
1329523	-6.966	-0.290
1020067	-6.957	-0.316
768495	-6.918	-0.231
1370066	-6.918	-0.329
1355340	-6.902	-0.256
798191	-6.894	-0.238
688372	-6.893	-0.276
1399616	-6.892	-0.119
624005	-6.890	-0.255
1452804	-6.887	-0.125
1567767	-6.864	-0.245
1259345	-6.863	-0.381
1289570	-6.863	-0.381
1240910	-6.855	-0.137
1569172	-6.846	-0.326
783751	-6.846	-0.214
1400351	-6.845	-0.236
1402781	-6.841	-0.360
676596	-6.839	-0.221
1404306	-6.824	-0.136
307401	-6.817	-0.284
1021279	-6.814	-0.273
70977	-6.807	-0.142
1399081	-6.806	-0.148
704882	-6.804	-0.235
750901	-6.802	-0.262
1341365	-6.800	-0.243
1518718	-6.792	-0.219
1285991	-6.778	-0.357

1363341	-6.774	-0.169
947751	-6.774	-0.261
1282168	-6.770	-0.260
1447617	-6.768	-0.141
7740	-6.762	-0.138
221099	-6.760	-0.307
1285083	-6.757	-0.282
628389	-6.755	-0.260
744906	-6.747	-0.198
1006953	-6.743	-0.293
1020476	-6.742	-0.250
1361734	-6.741	-0.132
1332463	-6.740	-0.281
1364120	-6.738	-0.146
640324	-6.738	-0.241
629439	-6.737	-0.217
682144	-6.736	-0.157
127273	-6.735	-0.396
1216580	-6.734	-0.396
1137709	-6.728	-0.280
1403596	-6.722	-0.292
1279052	-6.721	-0.354
1329701	-6.718	-0.129
993998	-6.711	-0.305
962693	-6.703	-0.258
1361991	-6.702	-0.146
1392648	-6.698	-0.258
828902	-6.692	-0.304
828902	-6.683	-0.304
771612	-6.680	-0.267
585706	-6.679	-0.352
1568332	-6.678	-0.257
1225132	-6.677	-0.139

636466	-6.676	-0.267
599227	-6.675	-0.223
1416008	-6.673	-0.318
707689	-6.672	-0.247
636166	-6.670	-0.238
962292	-6.670	-0.238
781950	-6.668	-0.230
128313	-6.665	-0.392
1304357	-6.665	-0.370
987411	-6.665	-0.290
647744	-6.663	-0.267

4.4.2 **Molecular Dynamic (MD) simulation and MM/GBSA.** For the top 100 molecules found in the docking job, molecular dynamics simulations were run for 1 ns, 10 ns, and 100 ns, collecting 100 frames for each simulation. One hundred protein-ligand complex structures were taken from the trajectory files after the simulations were finished. All structures also had MM/GBSA calculations, and average values over all time periods were determined. The hit candidates that emerged from the three simulation rounds are listed in Table 8 with their ChEMBL IDs, docking scores, and MM/GBSA scores.

Table 8.

Top Hit Molecules of ChemB Library with P40 and Their MM/GBSA Scores.

Protein-Ligand complex	**Docking score (kcal/mol)**	**1ns MD-MM/GBSA (kcal/mol)**	**10ns MD-MM/GBSA (kcal/mol)**	**100ns MD-MM/GBSA (kcal/mol)**
1431691	-7.251	-76.0981	-82.8226	-77.9068
70977	-6.807	-79.8999	-77.5944	-72.6854
7740	-6.762	-96.2405	-89.8166	-101.5921

1364120	-6.738	-75.4630	-77.0586	-100.9302
1361991	-6.702	-82.8109	-84.5580	-95.1621

The following Figures (28-32) represent the binding pocket and the 2D interaction map for the five hit molecules.

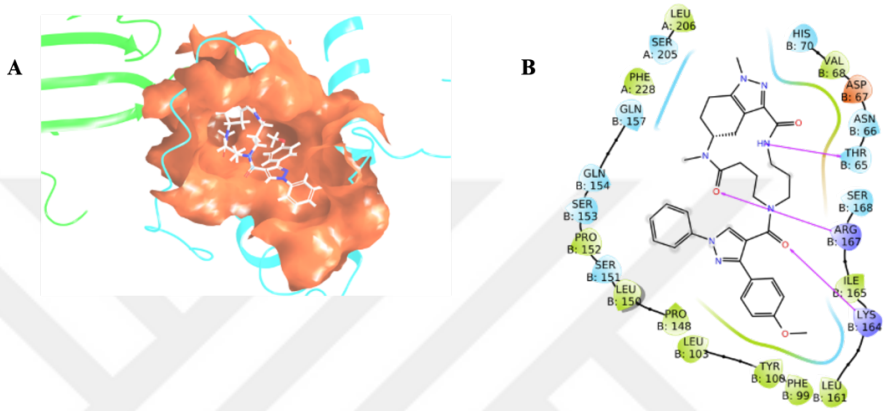

Figure 28. **A** Represent the P40/ 1431691 Binding Pocket. Where **B** Represent 2D Interaction Map of P40/ 1431691.

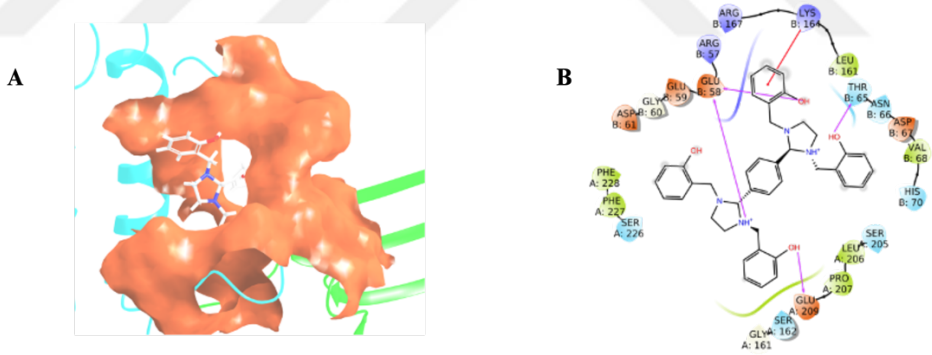

Figure 29. **A** Represent the P40/ 70977 Binding Pocket. Where **B** Represent 2D Interaction Map of P40/ 70977.

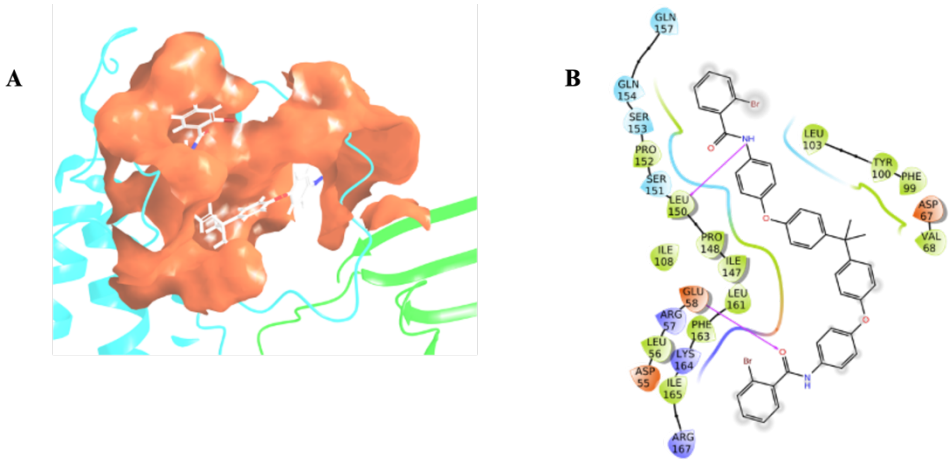

Figure 30. **A** Represent the P40/ 7740 Binding Pocket. Where **B** Represent 2D Interaction Map of P40/ 7740.

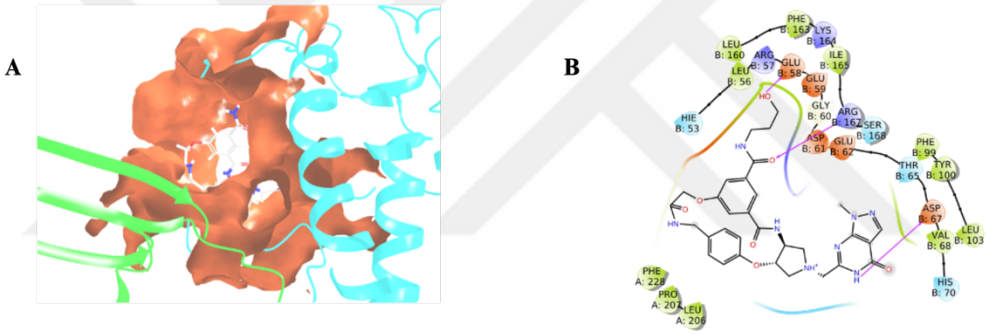

Figure 31. **A** Represent the P40/ 1364120 Binding Pocket. Where **B** Represent 2D Interaction Map of P40/ 1364120.

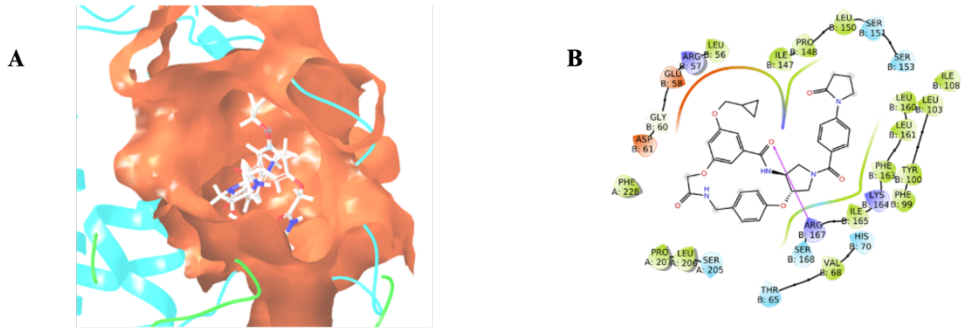

Figure 32. **A** Represent the P40/ 1361991 Binding Pocket. Where **B** Represent 2D Interaction Map of P40/ 1361991.

The purpose of the results presented in Table 8 and Figures (28-32) are to investigate the behavior of the ChEMBL ligands with IL-23p40 subunit over different MD

simulation's time with calculating the MM/GBSA in each step. The result of the ChEMBL ID 7740 which has the lowest MM/GBSA score in 100ns MD simulation, showed decreasing in the MM/GBSA when the simulation time had increased. Which means reaching -96.2405 kcal/mol on 1ns and increased to -101.5921 kcal/mol on 100ns, indicating increasing in the binding affinity and the stability of interaction between the ligand and protein over different time of the MD simulation. The ligand surface-interaction figures show the important reinduces binding with the ligand by hydrogen, hydrophobic bonds, and water bridge. In order to understand what that is mean, let's observe in Figure 34 the trajectory results of the best candidate in ChEMBL/ P40 simulations.

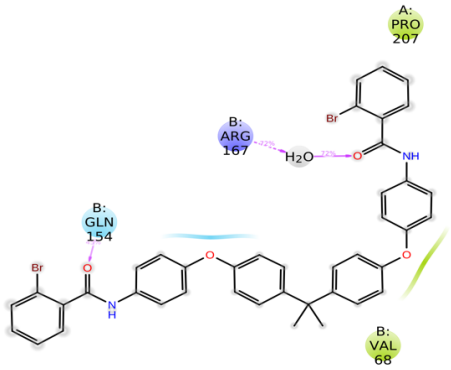

Figure 33. Ligand-Protein Contacts.

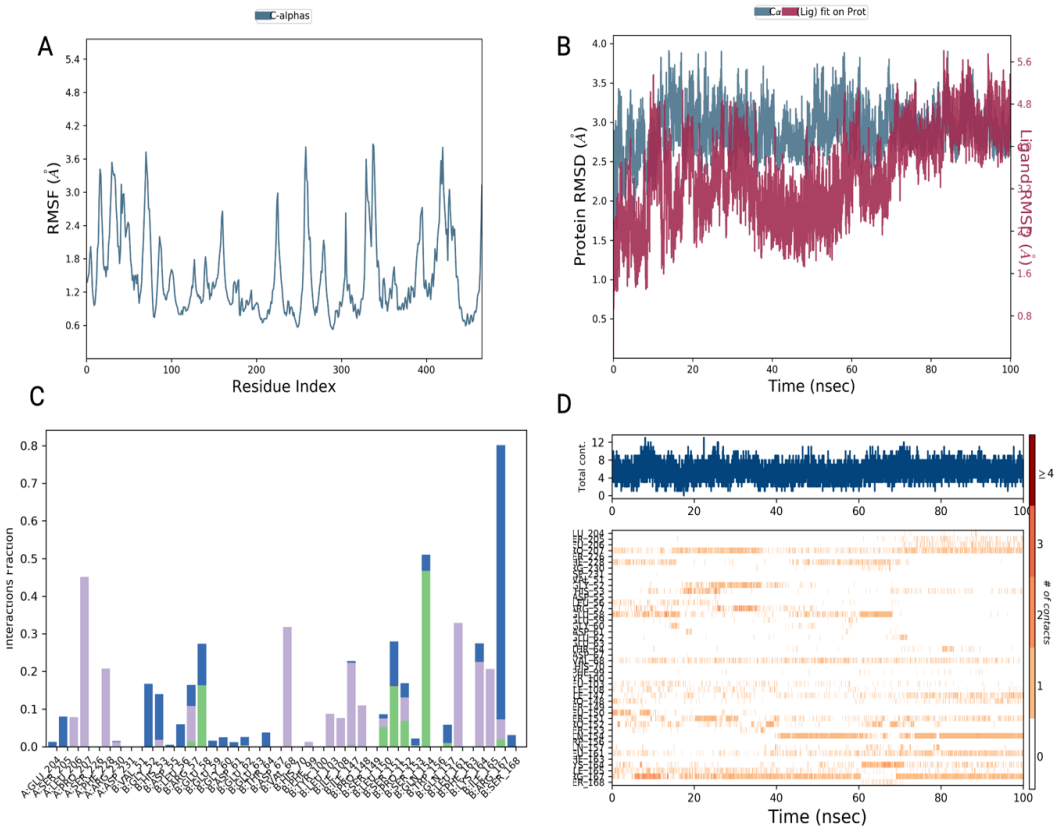

Figure 34. **A** Represent the RMSF, **B** Represent the RMSD, and **C** & **D** Represent the Protein-Ligand Contacts.

(Green, purple, and blue colours represent the H-bond, hydrophobic interaction, and water bridge respectively).

In Figure 34, A illustrates the root mean square fluctuation (RMSF) of the ChEMBL ID 7740, highlighting that the residues between amino acids 70-80, 200-280, 320-330, and 410-430 exhibit large fluctuations, where it ranges between 1.2 to 3.6 at most during the simulation. Where B depicts the root mean square deviation (RMSD), which measures the conformational changes of the protein and ligand structures throughout the simulation. The protein's RMSD values (left Y-axis) range from 2 to 3.5 Å, which is within the acceptable limits for RMSD measurements, indicating that the protein maintains structural stability. There is no jumping or large confirmational changes in RMSD which consider the fluctuations were within the acceptable limits. The ligand RMSD (right Y-axis) shows that the ligand remains slightly stable to the protein backbone and its binding

pocket. However, it showed higher fluctuations than the left Y-axis, where the values ranged from 1 to 3.5 Å. C and D provide insights into the protein-ligand contacts. Where C represent the histogram illustrates the distribution of various bonds throughout the simulation. Notably, a water bridge involving ARG167 is observed in 80% of the simulation time. Hydrophobic interactions are prominently present with residues such as PRO207, PHE228, VAL68, ILE147, PRO148, LEU161, LYS164, and ILE165. Additionally, a hydrogen bond is clearly identified with GLN154. Figure D also serves as a timeline representation of the interactions and contacts, corroborating the earlier findings. It highlights that some residues can form multiple specific contacts with the ligand. For instance, ARG167 and GLN154 display darker shades, indicating the presence of a water bridge and a hydrogen bond, respectively.

4.5 Result of the control groups comparing with the hit molecules

As of the date of this study, there is no FDA-approved small molecule inhibitor specifically targeting IL-23. Therefore, we compared three FDA-approved small molecule inhibitors—Deucravacitinib (a TYK2 inhibitor), Tofacitinib (a JAK inhibitor), and Brepocitinib (a dual TYK2 and JAK1 inhibitor)— against IL-23 hit inhibitors identified in our research. Although this comparison is not entirely accurate since the control groups do not directly target IL-23, it provides insight into some SMIs that treat psoriasis. The process involved several key steps. Initially, we prepared the ligands and performed docking studies for both the P19 and P40 subunits of IL-23 with the three inhibitors. Following the docking studies, we conducted molecular dynamics (MD) simulations, both 10 ns and 100 ns in duration, and calculated the molecular mechanics/generalized Born surface area (MM/GBSA) binding free energies. Then, we did QSAR models on the METACORE™/METADRUG™ platform to estimate their anti-psoriasis and skin disease activity score. Tables 9, 10 and 11 present the docking, MM/GBSA scores and QSAR scores for both P19 and P40, including the control groups alongside the hit molecules.

Table 9.

Top Hit Molecules with the Control Groups of P19.

P19 -Ligand complex	Docking score (kcal/mol)	10ns MD-MM/GBSA (kcal/mol)	100ns MD-MM/GBSA (kcal/mol)
Deucravacitinib	-4.635	-66.9716	-69.0856
Brepocitinib	-4.361	-40.1502	-38.7287
Tofacitinib	-4.361	-42.0393	-24.2689
Tenapanor	-7.248	-98.2585	-101.6643
360118	-7.94	-93.2946	-91.0027

Table 10.

Top Hit Molecules with the control Groups of P40.

P40-Ligand complex	Docking score (kcal/mol)	10ns MD-MM/GBSA (kcal/mol)	100ns MD-MM/GBSA (kcal/mol)
Deucravacitinib	-2.508	N/A	-58.5088
Brepocitinib	-3.071	N/A	-41.5509
Tofacitinib	-2.932	N/A	-22.3915
7740	-6.762	-96.2405	-101.5921

The docking results clearly indicate that the hit molecules identified in this study have significantly lower docking scores compared to the controls for both the P19 and P40 subunits which is completely clear since the control groups don't directly bind to IL-23. For example, Deucravacitinib, which achieved the best docking score among the control groups for both subunits, still has higher scores than all the candidate molecules. This underscores the efficiency and stability of the identified hit candidates. Additionally, an interesting observation is that the docking and MM/GBSA scores are markedly lower for P19 compared to P40 when considering the controls. Figures 35 and 36 also illustrate the

results of the 100 ns MD simulations of Deucravacitinib for the P19 and P40 subunits, respectively.

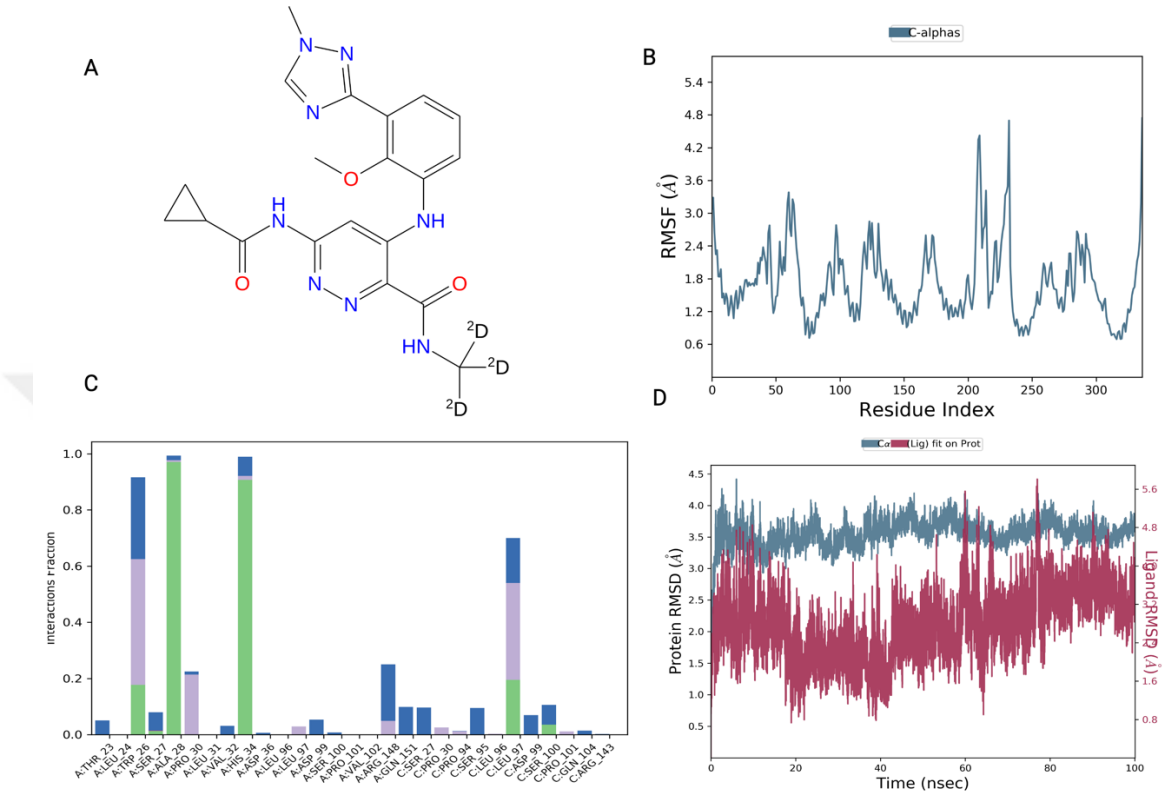

Figure 35. **A** 2D Structure of Deucravacitinib, **B** Represent the RMSF, **C** The P19-Ligand Contacts, and **D** Represent the RMSD.

(Green, purple, and blue colours represent the H-bond, hydrophobic interaction, and water bridge respectively).

Figure **A** depicts the 2D structure of Deucravacitinib, which comprises 53 atoms and has an atomic mass of 425.426 atomic units (au), with the molecular formula $C_{20}H_{22}N_8O_3$. Figure **B** illustrates the root mean square fluctuation (RMSF), indicating that the region between residues 200-250 fluctuates the most during the 100 ns simulation. Figure **C** shows the bonding interactions between the ligand and the protein, with hydrogen bonds clearly observed involving HIS34 and ALA28. Figure **D** displays the root mean square deviation (RMSD), indicating significant atomic displacement relative to the protein, suggesting that the ligand-protein structures are not well-fit and stable with each other.

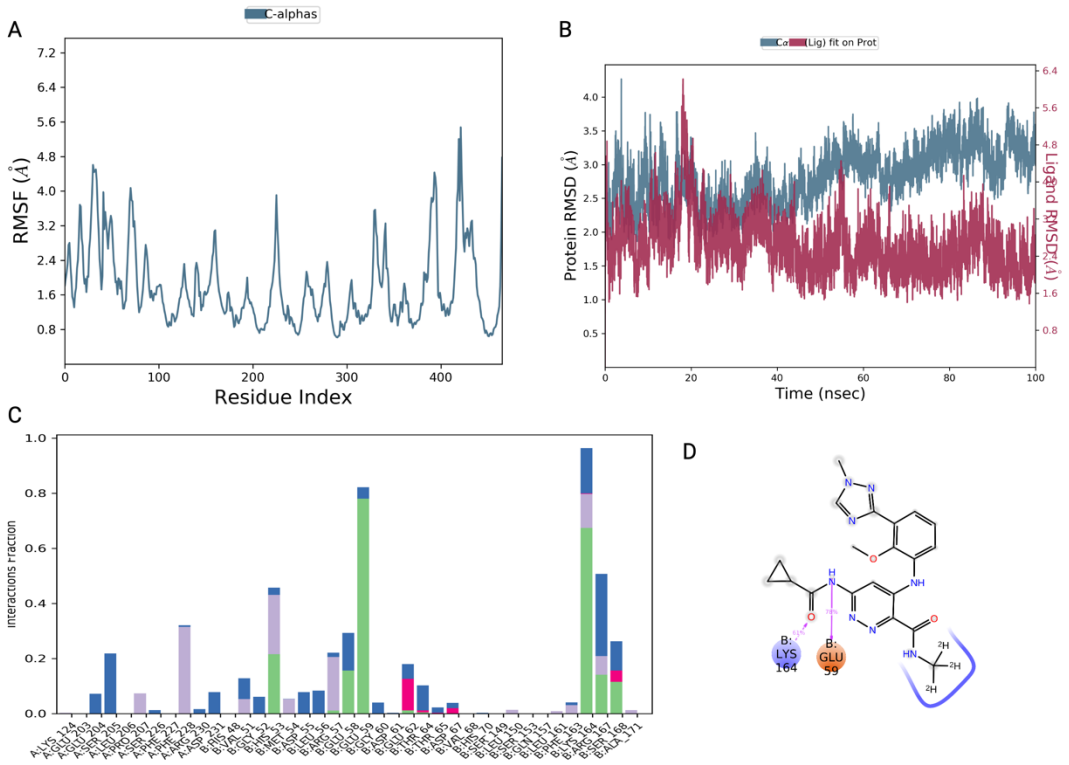

Figure 36. **A** represent the RMSF, **B** represent the RMSD, **C** represent the P40-ligand contacts, and **D** represent the ligand surface interaction.

(Green, purple, and blue colours represent the H-bond, hydrophobic interaction, and water bridge respectively).

Figure **A** represent the root mean square fluctuation (RMSF) of Deucravacitinib, indicating that the region between residues 200-250, 320-350 and 380-430 fluctuates the most during the 100 ns simulation. Figure **B** illustrates the root mean square deviation (RMSD) indicating significant atomic displacement relative to the protein, suggesting that the ligand-protein structures are not well-fit and stable with each other especially after 30ns. Figure **C** shows the bonding interactions between the ligand and the protein, with hydrogen bonds clearly observed involving HIS34 and ALA28. Figure **D** represents the ligand surface interaction between Deucravacitinib and the P40 of IL-23.

4.6 Result QSAR module and METACORE™/METADRUG™

To estimate the anti-psoriasis and skin disease activity score of Deucravacitinib and the identified inhibitors, the top compounds chosen from the 100ns MD and

MM/GBSA analysis of P19 and P40 of IL-23 were submitted to QSAR models on the METACORE™/METADRUG™ platform. The compounds with the highest score were found to have high anti-psoriasis and skin disease action. The cutoff value for the score was established at 0.5.

Table 11.

METACORE™/METADRUG™ scores.

2D structure	ID	MetaCore/Metadrug Psoriasis therapeutic activity	MetaCore/Metadrug skin disease therapeutic activity
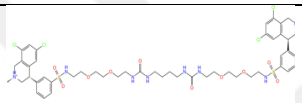	Tenapanor	0.34	0.21
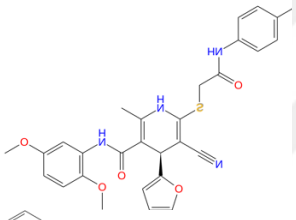	360118	0.42	0.54
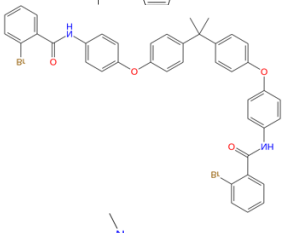	7740	0.27	0.76
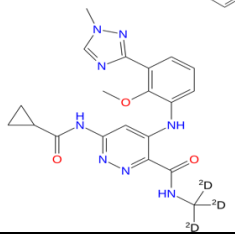	Deucravacitinb	0.38	0.36

Regarding the therapeutic activity for psoriasis, all of the hit molecules had cutoff values less than 0.5; however, the IDs 360118 and 7740 had cutoff values greater than 0.5, suggesting that they should be given additional consideration for investigation. Deucravacitinib, which is an FDA-approved medication for treating psoriasis, however, likewise displays a cutoff of 0.38 for skin disease and 0.36 for psoriasis, both of which are less than 0.5 and less than what is displayed for the ID 360118 and 7740.

Chapter 5: Discussion and Conclusion

5.1 Discussion

This thesis aims to use new methodology to screen large chemical databases (FDA database has 3.235 molecules and ChemBridge library has 1.569.617 molecules) to find small molecule inhibitors that can bind to either P19 or P40 of IL-23 which is central to the pathogenesis of psoriasis. Blocking the action of IL-23 could eventually limiting the inflammation that causes psoriasis and relieve the symptoms. Over the past few years, there has been an increasing in the use of IL-23 inhibitors to treat psoriasis, especially the biologic therapy where Risankizumab, Tildrakizumab, Guselkumab, (these are IL-23p19 inhibitors) and Ustekinumab (IL-23p40 inhibitor) are the main inhibitors of IL-23. However, none of the available FDA approved inhibitors are considered entirely satisfactory or ideal for psoriasis treatment and there is no small molecule inhibitor where directly target the IL-23.

Small molecule inhibitors (SMIs) offer several advantages over biologic treatments, including oral administration, a lower risk of immunogenic reactions, and reduced costs, making them more accessible and financially feasible. To explore the potential of SMIs for treating psoriasis, we initially docked IL-23p19 with the FDA database, generating the top 100 complexes based on their docking scores, which ranged from -8.548 kcal/mol to -6.182 kcal/mol. These 100 molecules were further refined through 1-ns MD simulations and MM/GBSA calculations, resulting in 10 promising candidates. These were then subjected to another 10-ns MD simulation with MM/GBSA calculations, narrowing the field to four molecules. A final 100-ns MD simulation and MM/GBSA calculations identified four hit molecules: Cobicistat, Indocyanine Green Acid Form, Lopinavir, and Tenapanor. Among these, Tenapanor emerged as the best option with a 100-ns MM/GBSA score of -101.6643 and a docking score of -6.389 kcal/mol. Tenapanor, an NHE3 inhibitor approved for treating constipation-predominant irritable bowel syndrome (IBS-C) and chronic kidney disease, showed promise initially (*Tenapanor*, n.d.). However, QSAR models on the METACORE™/METADRUG™ platform indicated that Tenapanor may not be effective for psoriasis and other skin

diseases, with therapeutic activity cutoffs of 0.32 and 0.21, respectively. Another inhibitor in this category that shows high potential for treating psoriasis is Indocyanine Green Acid, which achieved a docking score of -6.388 and exhibited relatively stable free energy calculations over three different time frames: -97.8199, -97.8902, and -97.2691 for 1ns, 10ns, and 100ns, respectively. This stability suggests a strong and reliable binding between Indocyanine Green Acid and IL-23p19 over time, reducing the risk of false positive results. In contrast, Tenapanor did not demonstrate this consistency, with free energy values of -98.2585, -86.9549, and -101.6643 over 1ns, 10ns, and 100ns MD simulations, respectively. The 100ns MD trajectory results for Tenapanor indicated that while the ligand remained stable with respect to the protein from 50ns to 100ns, there were structural conformation fluctuations exceeding 3 Å. This suggests that the protein undergoes significant conformational changes during the simulation according to the RMSF. Key residues identified as important in the interaction include PRO30, TRP26, SER100, ARG143, SER27, and ASP99, which engage in hydrogen bonding, hydrophobic interactions, and water bridge interactions, all of which are critical for drug specificity. Further investigation, including in vitro studies, is necessary to validate these findings and explore the therapeutic potential of these inhibitors.

The second set of results was obtained from docking IL-23p19 with the ChemBridge database, which comprises over 3 million small molecules. From the SP Glide docking, we selected the top 100 molecules based on their docking scores, which ranged from -9.634 kcal/mol to -7.524 kcal/mol, similar to the approach used with the FDA database. These 100 molecules were further filtered through 1-ns, 10-ns, and 100-ns MD simulations and MM/GBSA calculations, yielding five promising candidates with ChemBridge IDs: 1520093, 1242047, 1345219, 360118, and 1336950. Among these, ID 360118 demonstrated the best 100-ns MM/GBSA score of -91.0027, along with a docking score of -7.94. ID 360118 also exhibited stable MM/GBSA scores over different simulation times: -93.2946 at 1-ns, -92.8681 at 10-ns, and -91.0027 at 100-ns. Additionally, ID 360118 showed promising results in QSAR models on the METACORE™/METADRUG™ platform, with therapeutic activity scores of 0.42 and 0.54 for psoriasis and skin diseases, respectively. These findings highlight the potential of

ID 360118 as a promising candidate for further investigation and development as a therapeutic agent for psoriasis. Moreover, the 100-ns MD trajectory files revealed significant findings. The RMSD analysis indicated that the protein and ligand did not fit well together, with structural changes in the protein exceeding 5 Å. Despite this, three key residues—TRP26, LEU97, and SER100—exhibited notable interactions with the ligand throughout the simulation, including hydrogen bonds, hydrophobic interactions, and water bridge interactions. These interactions, although present, were insufficient to maintain the overall stability of the protein-ligand complex.

The third set of results was obtained from docking IL-23p40 with the FDA database. Using SP Glide docking, we selected the top 100 molecules based on their docking scores, which ranged from -7.686 kcal/mol to -4.999 kcal/mol, significantly lower than the docking scores for IL-23p19. Following a similar approach as with IL-23p19, these 100 molecules were further filtered through 1-ns, 10-ns, and 100-ns MD simulations and MM/GBSA calculations, resulting in five promising candidates: Piracetam, Propylthiouracil, Temozolomide, Hydroxyamphetamine, and Ephedrine. Among these, Temozolomide had the best 100-ns MM/GBSA score of -30.6036 and a docking score of -5.084. Which is an alkylating agent used to treat primary malignant brain tumours (*Temozolomide*, n.d.). However, it did not exhibit stable MM/GBSA scores over the simulation times of 1-ns, 10-ns, and 100-ns, showing -22.6925, -28.2721, and -30.6036, respectively, indicating significant variation during the simulation. Furthermore, analysis of the 100-ns MD trajectory files revealed that the ligand escaped the binding pocket, indicating the weak binding affinity, and unfavourable binding site, leading to the exclusion of Temozolomide from further investigation. These findings underscore the challenges of identifying stable and reliable inhibitors from IL-23 p40 and FDA database and the importance of consistent binding stability in candidate selection.

The final set of results was obtained from docking IL-23p40 with the ChemBridge database. Using SP Glide docking, we selected the top 100 molecules based on their docking scores, which ranged from -8.102 kcal/mol to -6.663 kcal/mol. Following our previously described approach, these 100 molecules were further filtered through 1-ns,

10-ns, and 100-ns MD simulations and MM/GBSA calculations, resulting in five promising candidates with ChemBridge IDs: 1431691, 70977, 7740, 1364120, and 1361991. Among these, ID 7740 demonstrated the best 100-ns MM/GBSA score of -101.5921 and a docking score of -6.762, comparable to the MM/GBSA results of Tenapanor. However, the MM/GBSA results for ID 7740 showed instability over the simulation time frames, with scores of -96.2405 at 1 ns, -89.8166 at 10 ns, and -101.5921 at 100 ns. Despite this, the 100-ns MD trajectory files indicated that the RMS deviation for this complex was the best fit between the protein and ligand among the other hits mentioned in this research, with a structural conformational change between 1 Å and 3.5 Å, which is considered acceptable over the 100-ns MD simulation. Crucial residues within the simulation, such as PRO207, VAL68, GLN154, and ARG167, showed strong interactions through hydrogen bonds, hydrophobic interactions, and water bridges. These interactions highlight the potential of ID 7740 as a promising candidate, although further in-vitro investigation is necessary to confirm its stability and efficacy to treat psoriasis. The QSAR models on the METACORE™/METADRUG™ platform indicated that this hit inhibitor exhibited the highest therapeutic activity for skin diseases with a score of 0.76, although it had a lower score of 0.27 for psoriasis. This makes it the most promising candidate for treating skin diseases among the hit molecules identified in this study.

The three hit molecules were compared with three small molecule inhibitors—Deucravacitinib, Brepocitinib, and Tofacitinib—that indirectly inhibit IL-23 by targeting either its downstream signalling pathways or other cytokines influencing IL-23 expression. SP Glide docking and 100-ns MD simulations were conducted for the control group with IL-23p19 and IL-23p40. Deucravacitinib demonstrated the best results with both subunits, achieving MM/GBSA scores of -69.0856 and -58.5088 and docking scores of -4.635 and -2.508, for IL-23p19 and IL-23p40 respectively. Although all the three hit molecules had lower docking and MM/GBSA scores than Deucravacitinib, but this's because that Deucravacitinib does not directly bind to the IL-23. However, when the hit molecules and Deucravacitinib were analysed using the METACORE™/METADRUG™ platform, Deucravacitinib exhibited lower therapeutic activity scores for psoriasis and skin diseases, with scores of 0.38 and 0.36, respectively. In contrast, the hit molecules

identified in this study demonstrated higher therapeutic potential. Despite Deucravacitinib being an approved small molecule inhibitor for treating psoriasis, these findings suggest that the hit molecules may offer more specific and effective therapeutic options for psoriasis. Further in-vitro investigations for Tenapanor, 7740, and 360118 is a must and a more in-depth analysis of molecule-binding interactions may require extended simulation durations.

5.2 Conclusion

In conclusion, our study aimed to repurpose small molecule inhibitors to treat moderate to severe psoriasis through high-throughput screening of large databases (FDA database and ChemBridge library). Initially, we performed docking for the FDA and ChemBridge databases separately with IL-23p19, selecting the top 100 complexes based on their docking scores. These top 100 complexes were then subjected to molecular dynamics (MD) simulations at three different time frames: 1 ns, 10 ns, and 100 ns. This process resulted in the identification of five hit molecules from each database. Among these, the best two hits, based on the 100 ns MM/GBSA results, were Tenapanor and ChemBridge ID 1336950. These findings highlight the potential of these small molecule inhibitors as promising therapeutic candidates for the treatment of moderate to severe psoriasis.

Subsequently, we performed docking for the FDA and ChemBridge databases separately with IL-23p40 also, selecting the top 100 complexes based on their docking scores. These top 100 complexes were subjected to molecular dynamics (MD) simulations at three different time frames: 1 ns, 10 ns, and 100 ns. This process resulted in the identification of five hit molecules from each database. And, the most promising hit, based on the 100 ns MM/GBSA results, was ChemBridge ID 7740, which showed comparable results to Tenapanor. Further comparative analysis between these two candidates is necessary to evaluate their psoriasis therapeutic potential fully.

The QSAR models on the METACORE™/METADRUG™ platform indicated that ChemBridge ID 7740 exhibited the highest therapeutic activity for skin diseases with a

score of 0.76, and ChemBridge ID 360118 showed a therapeutic activity score of 0.42 for psoriasis. These scores are notably higher than those of Deucravacitinib, a currently approved small molecule inhibitor for treating psoriasis, underscoring the potential of these identified hit molecules as more effective therapeutic options.

Chapter 6: Citations

Armstrong, A. W., & Read, C. (2020). Pathophysiology, Clinical Presentation, and Treatment of Psoriasis: A Review. *JAMA*, *323*(19), 1945. https://doi.org/10.1001/jama.2020.4006

Balak, D. M. W., Gerdes, S., Parodi, A., & Salgado-Boquete, L. (2020). Long-term Safety of Oral Systemic Therapies for Psoriasis: A Comprehensive Review of the Literature. *Dermatology and Therapy*, *10*(4), 589–613. https://doi.org/10.1007/s13555-020-00409-4

Bank, R. P. D. (n.d.). *RCSB PDB: Homepage*. Retrieved May 11, 2024, from https://www.rcsb.org/

Bellinato, F., Gisondi, P., & Girolomoni, G. (2021). Latest Advances for the Treatment of Chronic Plaque Psoriasis with Biologics and Oral Small Molecules. *Biologics: Targets and Therapy*, *15*, 247–253. https://doi.org/10.2147/BTT.S290309

Berekmeri, A., Mahmood, F., Wittmann, M., & Helliwell, P. (2018). Tofacitinib for the treatment of psoriasis and psoriatic arthritis. *Expert Review of Clinical Immunology*, *14*(9), 719–730. https://doi.org/10.1080/1744666X.2018.1512404

Berniyanti, T., Nugraha, A. P., Hidayati, N. N., Kharisma, V. D., Nugraha, A. P., & Noor, T. N. E. B. T. A. (2022). Computational study of Cu2+, Fe2+, Mn2+, Mn3+, Fe3+, CrO42-, Si4+, and Hg+ binding sites identification on cytokines to predict dental metal allergy: An in silico study. *Journal of Pharmacy & Pharmacognosy Research*, *10*(4), 687–694. https://doi.org/10.56499/jppres22.1372_10.4.687

Beyer, B. M., Ingram, R., Ramanathan, L., Reichert, P., Le, H. V., Madison, V., & Orth, P. (2008). Crystal Structures of the Pro-Inflammatory Cytokine Interleukin-23 and Its Complex with a High-Affinity Neutralizing Antibody. *Journal of Molecular Biology*, *382*(4), 942–955. https://doi.org/10.1016/j.jmb.2008.08.001

Bissonnette, R., Iversen, L., Sofen, H., Griffiths, C. E. M., Foley, P., Romiti, R., Bachinsky, M., Rottinghaus, S. T., Tan, H., Proulx, J., Valdez, H., Gupta, P., Mallbris, L., & Wolk, R. (2015). Tofacitinib withdrawal and retreatment in moderate-to-severe chronic plaque psoriasis: A randomized controlled trial. *The British Journal of Dermatology*, *172*(5), 1395–1406. https://doi.org/10.1111/bjd.13551

Blauvelt, A., Papp, K. A., Griffiths, C. E. M., Randazzo, B., Wasfi, Y., Shen, Y.-K., Li, S., & Kimball, A. B. (2017). Efficacy and safety of guselkumab, an anti-interleukin-23 monoclonal antibody, compared with adalimumab for the continuous treatment of patients with moderate to severe psoriasis: Results from the phase III, double-blinded, placebo- and active comparator-controlled VOYAGE 1 trial. *Journal of the American Academy of Dermatology*, *76*(3), 405–417. https://doi.org/10.1016/j.jaad.2016.11.041

Bloch, Y., Bouchareychas, L., Merceron, R., Składanowska, K., Bossche, L. V. den, Detry, S., Govindarajan, S., Elewaut, D., Haerynck, F., Dullaers, M., Adamopoulos, I. E., & Savvides, S. N. (2018). Structural Activation of Pro-inflammatory Human Cytokine IL-23 by Cognate IL-23 Receptor Enables Recruitment of the Shared Receptor IL-12Rβ1. *Immunity*, *48*(1), 45-58.e6. https://doi.org/10.1016/j.immuni.2017.12.008

Bowers, K. J., Chow, E., Xu, H., Dror, R. O., Eastwood, M. P., Gregersen, B. A., Klepeis, J. L., Kolossvary, I., Moraes, M. A., Sacerdoti, F. D., Salmon, J. K., Shan, Y., & Shaw, D. E. (2006). Scalable algorithms for molecular dynamics simulations on commodity clusters. *Proceedings of the 2006 ACM/IEEE Conference on Supercomputing*, 84-es. https://doi.org/10.1145/1188455.1188544

Camela, E., Ocampo-Garza, S. S., Cinelli, E., Villani, A., Fabbrocini, G., & Megna, M. (2021). Therapeutic update of biologics and small molecules for scalp psoriasis: A systematic review. *Dermatologic Therapy*, *34*(2), e14857. https://doi.org/10.1111/dth.14857

Caputo, V., Strafella, C., Cosio, T., Lanna, C., Campione, E., Novelli, G., Giardina, E., & Cascella, R. (2021). Pharmacogenomics: An Update on Biologics and Small-Molecule Drugs in the Treatment of Psoriasis. *Genes*, *12*(9), Article 9. https://doi.org/10.3390/genes12091398

Cascella, R., Strafella, C., Longo, G., Maccarone, M., Borgiani, P., Sangiuolo, F., Novelli, G., & Giardina, E. (2016). Pharmacogenomics of multifactorial diseases: A focus on psoriatic arthritis. *Pharmacogenomics*, *17*(8), 943–951. https://doi.org/10.2217/pgs.16.20

Chan, J. R., Blumenschein, W., Murphy, E., Diveu, C., Wiekowski, M., Abbondanzo, S., Lucian, L., Geissler, R., Brodie, S., Kimball, A. B., Gorman, D. M., Smith, K., de Waal Malefyt, R., Kastelein, R. A., McClanahan, T. K., & Bowman, E. P. (2006). IL-23 stimulates epidermal hyperplasia via TNF and IL-20R2–dependent mechanisms with implications for psoriasis pathogenesis. *Journal of Experimental Medicine*, *203*(12), 2577–2587. https://doi.org/10.1084/jem.20060244

Chen, I.-J., & Foloppe, N. (2010). Drug-like bioactive structures and conformational coverage with the LigPrep/ConfGen suite: Comparison to programs MOE and catalyst. *Journal of Chemical Information and Modeling*, *50*(5), 822–839. https://doi.org/10.1021/ci100026x

Chima, M., & Lebwohl, M. (2018). TNF inhibitors for psoriasis. *Seminars in Cutaneous Medicine and Surgery*, *37*(3), 134–142. https://doi.org/10.12788/j.sder.2018.039

Christophers, E. (2007). Comorbidities in psoriasis. *Clinics in Dermatology*, *25*(6), 529–534. https://doi.org/10.1016/j.clindermatol.2007.08.006

Colquhoun, M., & Kemp, A. K. (2024). Ustekinumab. In *StatPearls*. StatPearls Publishing. http://www.ncbi.nlm.nih.gov/books/NBK570645/

Cua, D. J., Sherlock, J., Chen, Y., Murphy, C. A., Joyce, B., Seymour, B., Lucian, L., To, W., Kwan, S., Churakova, T., Zurawski, S., Wiekowski, M., Lira, S. A., Gorman, D., Kastelein, R. A., & Sedgwick, J. D. (2003). Interleukin-23 rather than interleukin-12 is the critical cytokine for autoimmune inflammation of the brain. *Nature*, *421*(6924), 744–748. https://doi.org/10.1038/nature01355

Cytokine Frontiers. (n.d.). Retrieved May 8, 2024, from https://link.springer.com/book/10.1007/978-4-431-54442-5

Declerck, P. J., Darendeliler, F., Góth, M., Kolouskova, S., Micle, I., Noordam, C., Peterkova, V., Volevodz, N. N., Zapletalová, J., & Ranke, M. B. (2010). Biosimilars: Controversies as illustrated by rhGH. *Current Medical Research and Opinion*. https://doi.org/10.1185/03007991003719642

Dodson, J., & Lio, P. A. (2022). Biologics and Small Molecule Inhibitors: An Update in Therapies for Allergic and Immunologic Skin Diseases. *Current Allergy and Asthma Reports*, *22*(12), 183–193. https://doi.org/10.1007/s11882-022-01047-w

Dopytalska, K., Ciechanowicz, P., Wiszniewski, K., Szymańska, E., & Walecka, I. (2021). The Role of Epigenetic Factors in Psoriasis. *International Journal of Molecular Sciences*, *22*(17), 9294. https://doi.org/10.3390/ijms22179294

Ekins, S., Bugrim, A., Brovold, L., Kirillov, E., Nikolsky, Y., Rakhmatulin, E., Sorokina, S., Ryabov, A., Serebryiskaya, T., Melnikov, A., Metz, J., & Nikolskaya, T. (2006). Algorithms for network analysis in systems-ADME/Tox using the MetaCore and MetaDrug platforms. *Xenobiotica*, *36*(10–11), 877–901. https://doi.org/10.1080/00498250600861660

Essmann, U., Perera, L., Berkowitz, M. L., Darden, T., Lee, H., & Pedersen, L. G. (1995). A smooth particle mesh Ewald method. *The Journal of Chemical Physics*, *103*(19), 8577–8593. https://doi.org/10.1063/1.470117

Evans, D. J., & Holian, B. L. (1985). The Nose–Hoover thermostat. *The Journal of Chemical Physics*, *83*(8), 4069–4074. https://doi.org/10.1063/1.449071

Feldman, S. R., Goffe, B., Rice, G., Mitchell, M., Kaur, M., Robertson, D., Sierka, D., Bourret, J. A., Evans, T. S., & Gottlieb, A. (2016). The Challenge of Managing Psoriasis: Unmet Medical Needs and Stakeholder Perspectives. *American Health & Drug Benefits*, *9*(9), 504–513. https://www.ncbi.nlm.nih.gov/pmc/articles/PMC5394561/

Feldman, S. R., Thaçi, D., Gooderham, M., Augustin, M., Cruz, C. de la, Mallbris, L., Buonanno, M., Tatulych, S., Kaur, M., Lan, S., Valdez, H., & Mamolo, C. (2016).

Tofacitinib improves pruritus and health-related quality of life up to 52 weeks: Results from 2 randomized phase III trials in patients with moderate to severe plaque psoriasis. *Journal of the American Academy of Dermatology*, *75*(6), 1162-1170.e3. https://doi.org/10.1016/j.jaad.2016.07.040

Fiore, M., Leone, S., Maraolo, A. E., Berti, E., & Damiani, G. (2018). Liver Illness and Psoriatic Patients. *BioMed Research International*, *2018*, 3140983. https://doi.org/10.1155/2018/3140983

Forouzesh, N., & Mishra, N. (2021). An Effective MM/GBSA Protocol for Absolute Binding Free Energy Calculations: A Case Study on SARS-CoV-2 Spike Protein and the Human ACE2 Receptor. *Molecules*, *26*(8), 2383. https://doi.org/10.3390/molecules26082383

Friesner, R. A., Banks, J. L., Murphy, R. B., Halgren, T. A., Klicic, J. J., Mainz, D. T., Repasky, M. P., Knoll, E. H., Shelley, M., Perry, J. K., Shaw, D. E., Francis, P., & Shenkin, P. S. (2004). Glide: A New Approach for Rapid, Accurate Docking and Scoring. 1. Method and Assessment of Docking Accuracy. *Journal of Medicinal Chemistry*, *47*(7), 1739–1749. https://doi.org/10.1021/jm0306430

Friesner, R. A., Murphy, R. B., Repasky, M. P., Frye, L. L., Greenwood, J. R., Halgren, T. A., Sanschagrin, P. C., & Mainz, D. T. (2006). Extra precision glide: Docking and scoring incorporating a model of hydrophobic enclosure for protein-ligand complexes. *Journal of Medicinal Chemistry*, *49*(21), 6177–6196. https://doi.org/10.1021/jm051256o

Ghazawi, F. M., Mahmood, F., Kircik, L., Poulin, Y., Bourcier, M., Vender, R., Wiseman, M. C., Lynde, C., & Litvinov, I. V. (2021). A Review of the Efficacy and Safety

for Biologic Agents Targeting IL-23 in Treating Psoriasis With the Focus on Tildrakizumab. *Frontiers in Medicine*, *8*. https://doi.org/10.3389/fmed.2021.702776

Ghoreschi, K., Balato, A., Enerbäck, C., & Sabat, R. (2021). Therapeutics targeting the IL-23 and IL-17 pathway in psoriasis. *The Lancet*, *397*(10275), 754–766. https://doi.org/10.1016/S0140-6736(21)00184-7

Giordano, D., Biancaniello, C., Argenio, M. A., & Facchiano, A. (2022). Drug Design by Pharmacophore and Virtual Screening Approach. *Pharmaceuticals*, *15*(5), 646. https://doi.org/10.3390/ph15050646

Griffiths, C. E. M., Armstrong, A. W., Gudjonsson, J. E., & Barker, J. N. W. N. (2021a). Psoriasis. *The Lancet*, *397*(10281), 1301–1315. https://doi.org/10.1016/S0140-6736(20)32549-6

Griffiths, C. E. M., Armstrong, A. W., Gudjonsson, J. E., & Barker, J. N. W. N. (2021b). Psoriasis. *The Lancet*, *397*(10281), 1301–1315. https://doi.org/10.1016/S0140-6736(20)32549-6

Griffiths, C. E. M., Vender, R., Sofen, H., Kircik, L., Tan, H., Rottinghaus, S. T., Bachinsky, M., Mallbris, L., & Mamolo, C. (2017). Effect of tofacitinib withdrawal and re-treatment on patient-reported outcomes: Results from a Phase 3 study in patients with moderate to severe chronic plaque psoriasis. *Journal of the European Academy of Dermatology and Venereology: JEADV*, *31*(2), 323–332. https://doi.org/10.1111/jdv.13808

Griffiths Christopher E.M., Strober Bruce E., van de Kerkhof Peter, Ho Vincent, Fidelus-Gort Roseanne, Yeilding Newman, Guzzo Cynthia, Xia Yichuan, Zhou Bei, Li

Shu, Dooley Lisa T., Goldstein Neil H., & Menter Alan. (2010). Comparison of Ustekinumab and Etanercept for Moderate-to-Severe Psoriasis. *New England Journal of Medicine*, *362*(2), 118–128. https://doi.org/10.1056/NEJMoa0810652

Gulliver, W. P., Randell, S., Gulliver, S., Gregory, V., Nagle, S., & Chambenoit, O. (2018). Biologic Therapy Utilization in Patients With Moderate to Severe Psoriasis and Psoriatic Arthritis: An Observational Summary of Biologic Therapy Use in a Clinical Setting. *Journal of Cutaneous Medicine and Surgery*, *22*(6), 567–576. https://doi.org/10.1177/1203475418786712

Guo, J., Zhang, H., Lin, W., Lu, L., Su, J., & Chen, X. (2023). Signaling pathways and targeted therapies for psoriasis. *Signal Transduction and Targeted Therapy*, *8*(1), 1–38. https://doi.org/10.1038/s41392-023-01655-6

Halgren, T. A., Murphy, R. B., Friesner, R. A., Beard, H. S., Frye, L. L., Pollard, W. T., & Banks, J. L. (2004). Glide: A New Approach for Rapid, Accurate Docking and Scoring. 2. Enrichment Factors in Database Screening. *Journal of Medicinal Chemistry*, *47*(7), 1750–1759. https://doi.org/10.1021/jm030644s

Halim, S. A., Khan, A., Csuk, R., Al-Rawahi, A., & Al-Harrasi, A. (2020). Diterpenoids and Triterpenoids From Frankincense Are Excellent Anti-psoriatic Agents: An in silico Approach. *Frontiers in Chemistry*, *8*. https://doi.org/10.3389/fchem.2020.00486

Hansen, R. B., & Kavanaugh, A. (2014). Novel Treatments with Small Molecules in Psoriatic Arthritis. *Current Rheumatology Reports*, *16*(9), 443. https://doi.org/10.1007/s11926-014-0443-6

Harder, E., Damm, W., Maple, J., Wu, C., Reboul, M., Xiang, J. Y., Wang, L., Lupyan, D., Dahlgren, M. K., Knight, J. L., Kaus, J. W., Cerutti, D. S., Krilov, G., Jorgensen, W. L., Abel, R., & Friesner, R. A. (2016). OPLS3: A Force Field Providing Broad Coverage of Drug-like Small Molecules and Proteins. *Journal of Chemical Theory and Computation*, *12*(1), 281–296. https://doi.org/10.1021/acs.jctc.5b00864

Henseler, T., & Christophers, E. (1995). Disease concomitance in psoriasis. *Journal of the American Academy of Dermatology*, *32*(6), 982–986. https://doi.org/10.1016/0190-9622(95)91336-x

Hohenberger, M., Cardwell, L. A., Oussedik, E., & Feldman, S. R. (2018). Interleukin-17 inhibition: Role in psoriasis and inflammatory bowel disease. *Journal of Dermatological Treatment*, *29*(1), 13–18. https://doi.org/10.1080/09546634.2017.1329511

Igarashi, A., Kato, T., Kato, M., Song, M., Nakagawa, H., & Japanese Ustekinumab Study Group. (2012). Efficacy and safety of ustekinumab in Japanese patients with moderate-to-severe plaque-type psoriasis: Long-term results from a phase 2/3 clinical trial. *The Journal of Dermatology*, *39*(3), 242–252. https://doi.org/10.1111/j.1346-8138.2011.01347.x

Is psoriasis becoming more common? (2024, January 24). Psoriasis and Psoriatic Arthritis Alliance (PAPAA). https://www.papaa.org/news/current-features/is-psoriasis-becoming-more-common/

Jacobson, M. P., Pincus, D. L., Rapp, C. S., Day, T. J. F., Honig, B., Shaw, D. E., & Friesner, R. A. (2004). A hierarchical approach to all-atom protein loop prediction.

Proteins: Structure, Function, and Bioinformatics, *55*(2), 351–367. https://doi.org/10.1002/prot.10613

Jiang, Y., Chen, Y., Yu, Q., & Shi, Y. (2023). Biologic and Small-Molecule Therapies for Moderate-to-Severe Psoriasis: Focus on Psoriasis Comorbidities. *BioDrugs*, *37*(1), 35–55. https://doi.org/10.1007/s40259-022-00569-z

Jin, J. Q., Spencer, R. K., Reddy, V., Bhutani, T., & Liao, W. (2023). Clinical Utility of Deucravacitinib for the Management of Moderate to Severe Plaque Psoriasis. *Therapeutics and Clinical Risk Management*, *19*, 413–423. https://doi.org/10.2147/TCRM.S388324

Jorgensen, W. L., Chandrasekhar, J., Madura, J. D., Impey, R. W., & Klein, M. L. (1983). Comparison of simple potential functions for simulating liquid water. *The Journal of Chemical Physics*, *79*(2), 926–935. https://doi.org/10.1063/1.445869

Kamata, M., & Tada, Y. (2018). Safety of biologics in psoriasis. *The Journal of Dermatology*, *45*(3), 279–286. https://doi.org/10.1111/1346-8138.14096

Kamata, M., & Tada, Y. (2020). Efficacy and Safety of Biologics for Psoriasis and Psoriatic Arthritis and Their Impact on Comorbidities: A Literature Review. *International Journal of Molecular Sciences*, *21*(5), Article 5. https://doi.org/10.3390/ijms21051690

Kenny, P. W. (2019). The nature of ligand efficiency. *Journal of Cheminformatics*, *11*(1), 8. https://doi.org/10.1186/s13321-019-0330-2

Kwon, S., Bae, H., Jo, J., & Yoon, S. (2019). Comprehensive ensemble in QSAR prediction for drug discovery. *BMC Bioinformatics*, *20*(1), 521. https://doi.org/10.1186/s12859-019-3135-4

Langley, R. G., Tsai, T.-F., Flavin, S., Song, M., Randazzo, B., Wasfi, Y., Jiang, J., Li, S., & Puig, L. (2018). Efficacy and safety of guselkumab in patients with psoriasis who have an inadequate response to ustekinumab: Results of the randomized, double-blind, phase III NAVIGATE trial. *The British Journal of Dermatology*, *178*(1), 114–123. https://doi.org/10.1111/bjd.15750

Langrish, C. L., McKenzie, B. S., Wilson, N. J., De Waal Malefyt, R., Kastelein, R. A., & Cua, D. J. (2004). IL-12 and IL-23: Master regulators of innate and adaptive immunity. *Immunological Reviews*, *202*(1), 96–105. https://doi.org/10.1111/j.0105-2896.2004.00214.x

Lebwohl, M. g., Gordon, K. b., Gallo, G., Zhang, L., & Paul, C. (2020). Ixekizumab sustains high level of efficacy and favourable safety profile over 4 years in patients with moderate psoriasis: Results from UNCOVER-3 study. *Journal of the European Academy of Dermatology and Venereology*, *34*(2), 301–309. https://doi.org/10.1111/jdv.15921

Li, J., Abel, R., Zhu, K., Cao, Y., Zhao, S., & Friesner, R. A. (2011). The VSGB 2.0 model: A next generation energy model for high resolution protein structure modeling. *Proteins*, *79*(10), 2794–2812. https://doi.org/10.1002/prot.23106

Lønnberg, A. S., Skov, L., Skytthe, A., Kyvik, K. O., Pedersen, O. B., & Thomsen, S. F. (2013). Heritability of psoriasis in a large twin sample. *The British Journal of Dermatology*, *169*(2), 412–416. https://doi.org/10.1111/bjd.12375

Lowes, M. A., Bowcock, A. M., & Krueger, J. G. (2007). Pathogenesis and therapy of psoriasis. *Nature*, *445*(7130), 866–873. https://doi.org/10.1038/nature05663

Ma, C., Gu, C., Lian, P., Wazir, J., Lu, R., Ruan, B., Wei, L., Li, L., Pu, W., Peng, Z., Wang, W., Zong, Y., Huang, Z., Wang, H., Lu, Y., & Su, Z. (2023). Sulforaphane alleviates psoriasis by enhancing antioxidant defense through KEAP1-NRF2 Pathway activation and attenuating inflammatory signaling. *Cell Death & Disease*, *14*(11), 1–12. https://doi.org/10.1038/s41419-023-06234-9

Madhavaram, M., Nampally, V., Gangadhari, S., Palnati, M. K., & Tigulla, P. (2019). High-throughput virtual screening, ADME analysis, and estimation of MM/GBSA binding-free energies of azoles as potential inhibitors of Mycobacterium tuberculosis H37Rv. *Journal of Receptors and Signal Transduction*, *39*(4), 312–320. https://doi.org/10.1080/10799893.2019.1660895

Madhavi Sastry, G., Adzhigirey, M., Day, T., Annabhimoju, R., & Sherman, W. (2013). Protein and ligand preparation: Parameters, protocols, and influence on virtual screening enrichments. *Journal of Computer-Aided Molecular Design*, *27*(3), 221–234. https://doi.org/10.1007/s10822-013-9644-8

Makurvet, F. D. (2021). Biologics vs. small molecules: Drug costs and patient access. *Medicine in Drug Discovery*, *9*, 100075. https://doi.org/10.1016/j.medidd.2020.100075

Man, A.-M., Orăsan, M. S., Hoteiuc, O.-A., Olănescu-Vaida-Voevod, M.-C., & Mocan, T. (2023). Inflammation and Psoriasis: A Comprehensive Review. *International Journal of Molecular Sciences*, *24*(22), Article 22. https://doi.org/10.3390/ijms242216095

Martyna, G. J., Klein, M. L., & Tuckerman, M. (1992). Nosé–Hoover chains: The canonical ensemble via continuous dynamics. *The Journal of Chemical Physics*, *97*(4), 2635–2643. https://doi.org/10.1063/1.463940

Medicine Use and Spending in the U.S. (n.d.). Retrieved May 6, 2024, from https://www.iqvia.com/insights/the-iqvia-institute/reports-and-publications/reports/medicine-use-and-spending-in-the-us-review-of-2017-outlook-to-2022

Megino-Luque, C., Moiola, C. P., Molins-Escuder, C., López-Gil, C., Gil-Moreno, A., Matias-Guiu, X., Colas, E., & Eritja, N. (2020). Small-Molecule Inhibitors (SMIs) as an Effective Therapeutic Strategy for Endometrial Cancer. *Cancers*, *12*(10), 2751. https://doi.org/10.3390/cancers12102751

Mosca, M., Hong, J., Hadeler, E., Hakimi, M., Liao, W., & Bhutani, T. (2021). The Role of IL-17 Cytokines in Psoriasis. *ImmunoTargets and Therapy*, *10*, 409–418. https://doi.org/10.2147/ITT.S240891

Nair, P. A., & Badri, T. (2024). Psoriasis. In *StatPearls*. StatPearls Publishing. http://www.ncbi.nlm.nih.gov/books/NBK448194/

Naldi, L., & Mercuri, S. R. (2010). Epidemiology of comorbidities in psoriasis. *Dermatologic Therapy*, *23*(2), 114–118. https://doi.org/10.1111/j.1529-8019.2010.01304.x

Ogdie, A., Coates, L. C., & Gladman, D. D. (2020). Treatment guidelines in psoriatic arthritis. *Rheumatology (Oxford, England)*, *59*(Suppl 1), i37–i46. https://doi.org/10.1093/rheumatology/kez383

Papp, K. A., Menter, M. A., Abe, M., Elewski, B., Feldman, S. R., Gottlieb, A. B., Langley, R., Luger, T., Thaci, D., Buonanno, M., Gupta, P., Proulx, J., Lan, S., Wolk, R., & OPT Pivotal 1 and OPT Pivotal 2 investigators. (2015). Tofacitinib, an oral Janus kinase inhibitor, for the treatment of chronic plaque psoriasis: Results from two randomized, placebo-controlled, phase III trials. *The British Journal of Dermatology*, *173*(4), 949–961. https://doi.org/10.1111/bjd.14018

Parigi, T. L., Iacucci, M., & Ghosh, S. (2022). Blockade of IL-23: What is in the Pipeline? *Journal of Crohn's & Colitis*, *16*(Supplement_2), ii64–ii72. https://doi.org/10.1093/ecco-jcc/jjab185

Pastor-Fernández, G., Mariblanca, I. R., & Navarro, M. N. (2020). Decoding IL-23 Signaling Cascade for New Therapeutic Opportunities. *Cells*, *9*(9), 2044. https://doi.org/10.3390/cells9092044

Psoriasis—ScienceDirect. (n.d.). Retrieved April 21, 2024, from https://www.sciencedirect.com/science/article/abs/pii/S0140673620325496

PubChem. (n.d.). *Deucravacitinib*. Retrieved May 7, 2024, from https://pubchem.ncbi.nlm.nih.gov/compound/134821691

Raimondo, A., Balato, A., Megna, M., & Balato, N. (2018). Limitations of current monoclonal antibodies for plaque-type psoriasis and an outlook for the future. *Expert Opinion on Biological Therapy*, *18*(6), 605–607. https://doi.org/10.1080/14712598.2018.1479738

Reich, K., Armstrong, A. W., Foley, P., Song, M., Wasfi, Y., Randazzo, B., Li, S., Shen, Y.-K., & Gordon, K. B. (2017). Efficacy and safety of guselkumab, an anti-interleukin-23 monoclonal antibody, compared with adalimumab for the treatment

of patients with moderate to severe psoriasis with randomized withdrawal and retreatment: Results from the phase III, double-blind, placebo- and active comparator-controlled VOYAGE 2 trial. *Journal of the American Academy of Dermatology*, *76*(3), 418–431. https://doi.org/10.1016/j.jaad.2016.11.042

Reich, K., Papp, K. A., Blauvelt, A., Tyring, S. K., Sinclair, R., Thaçi, D., Nograles, K., Mehta, A., Cichanowitz, N., Li, Q., Liu, K., Rosa, C. L., Green, S., & Kimball, A. B. (2017). Tildrakizumab versus placebo or etanercept for chronic plaque psoriasis (reSURFACE 1 and reSURFACE 2): Results from two randomised controlled, phase 3 trials. *The Lancet*, *390*(10091), 276–288. https://doi.org/10.1016/S0140-6736(17)31279-5

Roos, K., Wu, C., Damm, W., Reboul, M., Stevenson, J. M., Lu, C., Dahlgren, M. K., Mondal, S., Chen, W., Wang, L., Abel, R., Friesner, R. A., & Harder, E. D. (2019). OPLS3e: Extending Force Field Coverage for Drug-Like Small Molecules. *Journal of Chemical Theory and Computation*, *15*(3), 1863–1874. https://doi.org/10.1021/acs.jctc.8b01026

Roskoski, R. (2023). Deucravacitinib is an allosteric TYK2 protein kinase inhibitor FDA-approved for the treatment of psoriasis. *Pharmacological Research*, *189*, 106642. https://doi.org/10.1016/j.phrs.2022.106642

Rowland, C. (2020, January 8). Why price of Humira keeps rising despite FDA approval of generic competition. *Washington Post*. https://www.washingtonpost.com/business/economy/why-humiras-price-keeps-rising-despite-fda-approval-of-generic-competition/2020/01/07/549ed0ce-2e3a-11ea-bcb3-ac6482c4a92f_story.html

Sawyer, L. M., Malottki, K., Sabry-Grant, C., Yasmeen, N., Wright, E., Sohrt, A., Borg, E., & Warren, R. B. (2019). Assessing the relative efficacy of interleukin-17 and interleukin-23 targeted treatments for moderate-to-severe plaque psoriasis: A systematic review and network meta-analysis of PASI response. *PLOS ONE*, *14*(8), e0220868. https://doi.org/10.1371/journal.pone.0220868

Sbidian, E., Chaimani, A., Guelimi, R., Garcia-Doval, I., Hua, C., Hughes, C., Naldi, L., Kinberger, M., Afach, S., & Cleach, L. L. (2023). Systemic pharmacological treatments for chronic plaque psoriasis: A network meta-analysis. *Cochrane Database of Systematic Reviews*, *7*. https://doi.org/10.1002/14651858.CD011535.pub6

Scher, J. U., Ubeda, C., Artacho, A., Attur, M., Isaac, S., Reddy, S. M., Marmon, S., Neimann, A., Brusca, S., Patel, T., Manasson, J., Pamer, E. G., Littman, D. R., & Abramson, S. B. (2015). Decreased Bacterial Diversity Characterizes an Altered Gut Microbiota in Psoriatic Arthritis and Resembles Dysbiosis of Inflammatory Bowel Disease. *Arthritis & Rheumatology (Hoboken, N.J.)*, *67*(1), 128–139. https://doi.org/10.1002/art.38892

Shelley, J. C., Cholleti, A., Frye, L. L., Greenwood, J. R., Timlin, M. R., & Uchimaya, M. (2007). Epik: A software program for pK(a) prediction and protonation state generation for drug-like molecules. *Journal of Computer-Aided Molecular Design*, *21*(12), 681–691. https://doi.org/10.1007/s10822-007-9133-z

Sherlock, J. P., & Cua, D. J. (2021). Interleukin-23 in perspective. *Rheumatology*, *60*(Supplement_4), iv1–iv3. https://doi.org/10.1093/rheumatology/keab461

Sherlock, J. P., Joyce-Shaikh, B., Turner, S. P., Chao, C.-C., Sathe, M., Grein, J., Gorman, D. M., Bowman, E. P., McClanahan, T. K., Yearley, J. H., Eberl, G., Buckley, C. D., Kastelein, R. A., Pierce, R. H., LaFace, D. M., & Cua, D. J. (2012). IL-23 induces spondyloarthropathy by acting on ROR-γt+ CD3+CD4−CD8− entheseal resident T cells. *Nature Medicine*, *18*(7), 1069–1076. https://doi.org/10.1038/nm.2817

Sivamani, R. K., Correa, G., Ono, Y., Bowen, M. P., Raychaudhuri, S. P., & Maverakis, E. (2010). BIOLOGICAL THERAPY OF PSORIASIS. *Indian Journal of Dermatology*, *55*(2), 161–170. https://doi.org/10.4103/0019-5154.62754

Song, C., Yang, C., Meng, S., Li, M., Wang, X., Zhu, Y., Kong, L., Lv, W., Qiao, H., & Sun, Y. (2021). Deciphering the mechanism of Fang-Ji-Di-Huang-Decoction in ameliorating psoriasis-like skin inflammation via the inhibition of IL-23/Th17 cell axis. *Journal of Ethnopharmacology*, *281*, 114571. https://doi.org/10.1016/j.jep.2021.114571

Suzuki, E., Mellins, E. D., Gershwin, M. E., Nestle, F. O., & Adamopoulos, I. E. (2014). The IL-23/IL-17 axis in psoriatic arthritis. *Autoimmunity Reviews*, *13*(4–5), 496–502. https://doi.org/10.1016/j.autrev.2014.01.050

Tang, C., Chen, S., Qian, H., & Huang, W. (2012). Interleukin-23: As a drug target for autoimmune inflammatory diseases. *Immunology*, *135*(2), 112–124. https://doi.org/10.1111/j.1365-2567.2011.03522.x

Temozolomide. (n.d.). Retrieved June 30, 2024, from https://go.drugbank.com/drugs/DB00853

Tenapanor. (n.d.). Retrieved June 30, 2024, from https://go.drugbank.com/drugs/DB11761

Teunissen, M. B. M., Bos, J. D., Koomen, C. W., de Waal Malefyt, R., & Wierenga, E. A. (1998). Interleukin-17 and Interferon-γ Synergize in the Enhancement of Proinflammatory Cytokine Production by Human Keratinocytes. *Journal of Investigative Dermatology*, *111*(4), 645–649. https://doi.org/10.1046/j.1523-1747.1998.00347.x

Thakur, S., Anjum, M. M., Jaiswal, S., Gautam, A. K., & Rajinikanth, P. S. (2023). Tazarotene-calcipotriol loaded Nanostructured lipid carrier enriched hydrogel: A novel dual drug synergistic approach towards Psoriasis management. *Journal of Drug Delivery Science and Technology*, *88*, 104944. https://doi.org/10.1016/j.jddst.2023.104944

Tian, F., Chen, Z., & Xu, T. (2019). Efficacy and safety of tofacitinib for the treatment of chronic plaque psoriasis: A systematic review and meta-analysis. *The Journal of International Medical Research*, *47*(6), 2342–2350. https://doi.org/10.1177/0300060519847414

Torres, T., & Filipe, P. (2015a). Small Molecules in the Treatment of Psoriasis. *Drug Development Research*, *76*(5), 215–227. https://doi.org/10.1002/ddr.21263

Torres, T., & Filipe, P. (2015b). Small Molecules in the Treatment of Psoriasis. *Drug Development Research*, *76*(5), 215–227. https://doi.org/10.1002/ddr.21263

Truong, T. M., Pathak, G. N., Singal, A., Taranto, V., & Rao, B. K. (2024). Deucravacitinib: The First FDA-Approved Oral TYK2 Inhibitor for Moderate to

Severe Plaque Psoriasis. *Annals of Pharmacotherapy*, *58*(4), 416–427. https://doi.org/10.1177/10600280231153863

Tsai, T.-F., Ho, J.-C., Song, M., Szapary, P., Guzzo, C., Shen, Y.-K., Li, S., Kim, K.-J., Kim, T.-Y., Choi, J.-H., Youn, J.-I., & PEARL Investigators. (2011). Efficacy and safety of ustekinumab for the treatment of moderate-to-severe psoriasis: A phase III, randomized, placebo-controlled trial in Taiwanese and Korean patients (PEARL). *Journal of Dermatological Science*, *63*(3), 154–163. https://doi.org/10.1016/j.jdermsci.2011.05.005

Turner, S. (2018, September 5). Humira: The highs and lows of the world's most successful drug. *Pharmaceutical Technology*. https://www.pharmaceutical-technology.com/features/humira-abbvie-drug/

Vilar, S., & Costanzi, S. (2012). Predicting Biological Activities through QSAR Analysis and Docking-based Scoring. *Methods in Molecular Biology (Clifton, N.J.)*, *914*, 271–284. https://doi.org/10.1007/978-1-62703-023-6_16

Yang, K., Oak, A. S. W., & Elewski, B. E. (2021). Use of IL-23 Inhibitors for the Treatment of Plaque Psoriasis and Psoriatic Arthritis: A Comprehensive Review. *American Journal of Clinical Dermatology*, *22*(2), 173–192. https://doi.org/10.1007/s40257-020-00578-0

Yen, D., Cheung, J., Scheerens, H., Poulet, F., McClanahan, T., Mckenzie, B., Kleinschek, M. A., Owyang, A., Mattson, J., Blumenschein, W., Murphy, E., Sathe, M., Cua, D. J., Kastelein, R. A., & Rennick, D. (2006). IL-23 is essential for T cell–mediated colitis and promotes inflammation via IL-17 and IL-6. *The Journal of Clinical Investigation*, *116*(5), 1310–1316. https://doi.org/10.1172/JCI21404

Zhang, W., Bell, E. W., Yin, M., & Zhang, Y. (2020). EDock: Blind protein–ligand docking by replica-exchange monte carlo simulation. *Journal of Cheminformatics*, *12*(1), 37. https://doi.org/10.1186/s13321-020-00440-9

Zhou, X., Chen, Y., Cui, L., Shi, Y., & Guo, C. (2022). Advances in the pathogenesis of psoriasis: From keratinocyte perspective. *Cell Death & Disease*, *13*(1), 1–13. https://doi.org/10.1038/s41419-022-04523-3

Zhu, X., Zheng, M., Song, M., Shen, Y.-K., Chan, D., Szapary, P. O., Wang, B., & LOTUS Investigators. (2013). Efficacy and safety of ustekinumab in Chinese patients with moderate to severe plaque-type psoriasis: Results from a phase 3 clinical trial (LOTUS). *Journal of Drugs in Dermatology: JDD*, *12*(2), 166–174.